Developmental Biology 365 (2012) 36–49

Contents lists available at SciVerse ScienceDirect

Developmental Biology

journal homepage: www.elsevier.com/developmentalbiology

Multiple Slits regulate the development of midline glial populations and the corpus callosum

Divya K. Unni [a], Michael Piper [a,b], Randal X. Moldrich [a,c], Ilan Gobius [a], Sha Liu [a], Thomas Fothergill [a,1], Amber-Lee S. Donahoo [a], John M. Baisden [a], Helen M. Cooper [a,b], Linda J. Richards [a,b,*]

[a] The Queensland Brain Institute, The University of Queensland, Brisbane 4072, Australia
[b] The School of Biomedical Sciences, The University of Queensland, Brisbane 4072, Australia
[c] The Centre for Advanced Imaging, The University of Queensland, Brisbane 4072, Australia

ARTICLE INFO

Article history:
Received for publication 2 June 2011
Revised 20 January 2012
Accepted 3 February 2012
Available online 11 February 2012

Keywords:
Indusium griseum glia
Axon guidance
Midline formation
Cerebral cortex
Diffusion magnetic resonance imaging
Commissure formation

ABSTRACT

The Slit molecules are chemorepulsive ligands that regulate axon guidance at the midline of both vertebrates and invertebrates. In mammals, there are three *Slit* genes, but only *Slit2* has been studied in any detail with regard to mammalian brain commissure formation. Here, we sought to understand the relative contributions that *Slit* proteins make to the formation of the largest brain commissure, the corpus callosum. Slit ligands bind Robo receptors, and previous studies have shown that *Robo1*$^{-/-}$ mice have defects in corpus callosum development. However, whether the *Slit* genes signal exclusively through *Robo1* during callosal formation is unclear. To investigate this, we compared the development of the corpus callosum in both *Slit2*$^{-/-}$ and *Robo1*$^{-/-}$ mice using diffusion magnetic resonance imaging. This analysis demonstrated similarities in the phenotypes of these mice, but crucially also highlighted subtle differences, particularly with regard to the guidance of post-crossing axons. Analysis of single mutations in *Slit* family members revealed corpus callosum defects (but not complete agenesis) in 100% of *Slit2*$^{-/-}$ mice and 30% of *Slit3*$^{-/-}$ mice, whereas 100% of *Slit1*$^{-/-}$; *Slit2*$^{-/-}$ mice displayed complete agenesis of the corpus callosum. These results revealed a role for *Slit1* in corpus callosum development, and demonstrated that *Slit2* was necessary but not sufficient for midline crossing *in vivo*. However, co-culture experiments utilising *Robo1*$^{-/-}$ tissue versus Slit2 expressing cell blocks demonstrated that Slit2 was sufficient for the guidance activity mediated by Robo1 in pre-crossing neocortical axons. This suggested that Slit1 and Slit3 might also be involved in regulating other mechanisms that allow the corpus callosum to form, such as the establishment of midline glial populations. Investigation of this revealed defects in the development and dorso-ventral positioning of the indusium griseum glia in multiple *Slit* mutants. These findings indicate that *Slits* regulate callosal development via both classical chemorepulsive mechanisms, and via a novel role in mediating the correct positioning of midline glial populations. Finally, our data also indicate that some of the roles of Slit proteins at the midline may be independent of Robo signalling, suggestive of additional receptors regulating Slit signalling during development.

Background

The corpus callosum is the largest axon tract in the brain, yet the molecular mechanisms regulating its formation remain poorly understood. The corpus callosum is made up of axons from neurons predominantly located in layers II, III and V of the neocortex. These neurons extend axons across the cortical midline via the corpus callosum and into the contralateral hemisphere, where they form homotopic connections (Wise and Jones, 1976). In humans, the rostral (rostrum and genu) and middle (body) regions of the corpus callosum develop embryonically, whereas the caudal (splenium) corpus callosum develops largely during the perinatal period through to adolescence (Paul et al., 2007). In mice, formation of the corpus callosum is initiated at approximately embryonic day 16 (E16) and concludes around postnatal day 15 (P15; Ozaki and Wahlsten, 1992; Richards, 2002). The environment through which callosal axons navigate during the formation of the corpus callosum is complex, with a number of different axonal guidance families implicated in regulating their guidance, including members of the Slit, Semaphorin, Wnt, and Ephrin families, as well as Draxin (Bagri et al., 2002; Islam et al., 2009; Keeble et al., 2006; Mendes et al., 2006; Niquille et al., 2009; Piper et al., 2009b; Shu and Richards, 2001).

* Corresponding author at: NHMRC Principal Research Fellow, Head, Cortical Development and Axon Guidance Laboratory, The Queensland Brain Institute and The School of Biomedical Sciences, The University of Queensland, Brisbane 4072, Australia. Fax: +61 7 33466301.
E-mail addresses: divya.unni@gmail.com (D.K. Unni), m.piper@uq.edu.au (M. Piper), r.moldrich@uq.edu.au (R.X. Moldrich), i.gobius@uq.edu.au (I. Gobius), sha.liu@uqconnect.edu.au (S. Liu), tfothergill@wisc.edu (T. Fothergill), a.donahoo@uq.edu.au (A.-L.S. Donahoo), j.baisden@uq.edu.au (J.M. Baisden), h.cooper@uq.edu.au (H.M. Cooper), richards@uq.edu.au (L.J. Richards).
[1] Current address: University of Wisconsin-Madison, Department of Neuroscience, Madison, WI 53706, USA.

0012-1606/$ – see front matter © 2012 Elsevier Inc. All rights reserved.
doi:10.1016/j.ydbio.2012.02.004

The *Slit* genes are an evolutionarily conserved group of chemorepulsive axon guidance molecules. *Slit2*$^{-/-}$ mice exhibit a variety of axon guidance anomalies, including abnormal development of the thalamocortical, corticofugal, optic, and olfactory tracts (Bagri et al., 2002; Nguyen-Ba-Charvet et al., 2002; Plump et al., 2002). *Slit2*$^{-/-}$ mice also exhibit callosal dysgenesis (Bagri et al., 2002); however a comprehensive investigation into the callosal phenotype of these mice has so far been lacking, and whether *Slit1*$^{-/-}$ or *Slit3*$^{-/-}$ mice have defects in callosal development remains unknown. Slit-mediated chemorepulsion occurs via Slit binding to members of the Robo family of transmembrane receptors (Brose et al., 1999; Kidd et al., 1999). Robo1 in particular has been implicated in the development of the corpus callosum (Andrews et al., 2006; Lopez-Bendito et al., 2007), and is thought to be responsible for transducing Slit signalling within callosal axons. However, whether *Robo1*$^{-/-}$ mice phenocopy *Slit2*$^{-/-}$ mice with respect to callosal development has not been thoroughly investigated.

In addition to extracellular guidance cues, the formation of axon tracts during development is also reliant on glial populations located at key choice points along the trajectory of navigating axons. For instance, midline glial populations are associated with commissural projections in the brain and spinal cord and their role in regulating commissural development has been conserved throughout evolution. Midline glia play a crucial role in callosal formation through the expression of guidance molecules such as Slit, Wnt, Draxin, bone morphogenetic protein (BMP) 7 and Ephrins (Bagri et al., 2002; Islam et al., 2009; Keeble et al., 2006; Mendes et al., 2006; Sánchez-Camacho et al., 2011; Shu and Richards, 2001). At the developing telencephalic midline, three midline glial populations have been characterised: the glial wedge, the indusium griseum glia and the midline zipper glia (Shu et al., 2003b; Silver et al., 1993). Cells within the glial wedge and indusium griseum glia express *Slit2* (Shu and Richards, 2001), which has been shown to play a role in the guidance of callosal axons approaching the cortical midline, and those that have already crossed the midline (Shu et al., 2003c). In addition, BMP7 has been shown to regulate the development of both corridor neurons and glia at the cortical midline (Sánchez-Camacho et al., 2011). Transcription factors such as the nuclear factor one proteins regulate the differentiation of glial populations at the cortical midline (Piper et al., 2009a, 2010; Shu et al., 2003a) but little is known about how dorsoventral positioning of these glial populations is co-ordinated during development. Importantly, Slit expression has been shown to contribute to the positioning of glial cells in the developing midline of the zebrafish forebrain (Barresi et al., 2005). However, whether expression of Slit proteins at the telencephalic midline plays an analogous role is still to be determined.

Here we address some of these outstanding issues with regard to callosal development. Specifically, we present a comprehensive analysis of the roles of *Slit1*, *Slit2* and *Slit3* during corpus callosum formation. Moreover, we demonstrate that *Slit2*$^{-/-}$ mice have a more severe callosal phenotype than *Robo1*$^{-/-}$ mice, indicating a role for additional receptors in this system, and that *Slit* mutants display defects in the positioning of glial populations at the cortical midline. These data provide a significant advance in our understanding of the molecular determinants of callosal formation, and reveal a previously unsuspected role for *Slit* genes in regulating the position of crucial glial populations at the midline of the mammalian brain.

Results

Expression of Slits and Robos at the developing cortical midline

The *Slit* genes are widely expressed within the developing rodent telencephalon (Marillat et al., 2002), and we have previously shown that *Slit2* is expressed within the glial wedge and indusium griseum on E17 in the mouse cortex (Shu and Richards, 2001). However, neither the expression of *Slit1* and *Slit3* at the cortical midline in mouse, nor the expression of *Slit2* at E16, when the trajectory of the corpus callosum is first established, had previously been analysed in detail. Using *in situ* hybridisation, we analysed the expression of each *Slit* family member at E16 and compared their expression patterns. In the septum and cortical plate, *Slit1* was most highly expressed (compare Fig. 1A, A′″ with Fig. 1B and C and B′″ and C′″, respectively). *Slit3* was expressed at very low levels in the cortical plate (Fig. 1C′″). To examine Slit expression within the midline glial populations we immunohistochemically co-labelled our *in situ* hybridisation samples for anti-glial fibrillary acidic protein (GFAP). However, as this antibody does not label the cytoplasm of glia, only regional, rather than cellular, co-localisation was possible. The results indicated that *Slit2* expression overlapped with GFAP labelling within the indusium griseum (Fig. 1B′) whereas, although both *Slit1* and *Slit3* were expressed in the indusium griseum, their expression did not overlap with that of GFAP (Fig. 1A′ and B′ respectively). All three *Slit* molecules were expressed in the glial wedge (Fig. 1A″, B″, C″).

We next examined the midline glial populations in sagittal view in relation to their proximity to the commissural tracts present in this region (Fig. 2A, A′). This plane of section revealed that the indusium griseum glia wrap around the dorsal aspect of the corpus callosum and represent an extensive glial population (arrowheads in Fig. 2A′). However, when the glial wedge were stained in sagittal sections they were difficult to delineate because their glial processes, which run from lateral to medial, had been cut in cross-section (arrow Fig. 1A′). Given that *Slit2* expression overlapped with GFAP in our initial analysis we wanted to examine its expression in sagittal sections where the rostro-caudal extent of the indusium griseum can be appreciated. We found that *Slit2* expression overlapped with GFAP expression in the indusium griseum from rostral to caudal but was higher caudally (Fig. 2B, B′, arrow in B″).

The expression of Robo1 and Robo2 has previously been described in the mouse cortex (Shu and Richards, 2001), but their expression in midline glial populations has not been addressed. To investigate this we used *in situ* hybridisation probes against *Robo1* and *Robo2*, co-labelled with anti-GFAP as above. *Robo1* and *Robo2* were expressed in the cortical plate (Fig. 3A′″, B′″) as previously described (Shu and Richards, 2001), but did not co-localise with GFAP in the cortex at this stage. In the midline glial populations, both *Robos* were expressed in the indusium griseum but were not expressed in the GFAP-positive population (Fig. 3A′ and B′), and only *Robo1* was expressed in the ventral glial wedge (Fig. 3A″, B″).

In summary, the indusium griseum expresses all three *Slits* and *Robo1* and *Robo2*, but only *Slit2* is expressed in the glial cells of the indusium griseum. In the glial wedge, all three *Slits* and *Robo1* are expressed in the GFAP-positive population.

Slit genes regulate the development of the corpus callosum

To investigate the role of the *Slit* genes in corpus callosum development, we analysed the formation of this tract in mice lacking *Slit1*, *Slit2* or *Slit3* at E17, the age at which neocortical callosal axons begin to cross the cortical midline (Ozaki and Wahlsten, 1992). Immunohistochemistry against the axonal marker GAP43 revealed no defects in the formation of the corpus callosum in *Slit1*$^{-/-}$ mice (Fig. 4D–F), despite the expression of this gene in the indusium griseum and septum (Figs. 1 and 2). In contrast, 100% of *Slit2*$^{-/-}$ mice exhibited defects in callosal formation at E17, in line with previous reports (Bagri et al., 2002). Although some axons crossed into the contralateral hemisphere via the corpus callosum in *Slit2*$^{-/-}$ mice, others stalled at the midline or coursed aberrantly into the septum (Fig. 4G–I). These data complement the tract-tracing studies previously performed on the *Slit2*$^{-/-}$ mice (Bagri et al., 2002), indicating that *Slit2* is necessary for callosal formation. In *Slit3*$^{-/-}$ mice we observed an acallosal phenotype in the rostral, but not caudal, regions of the corpus

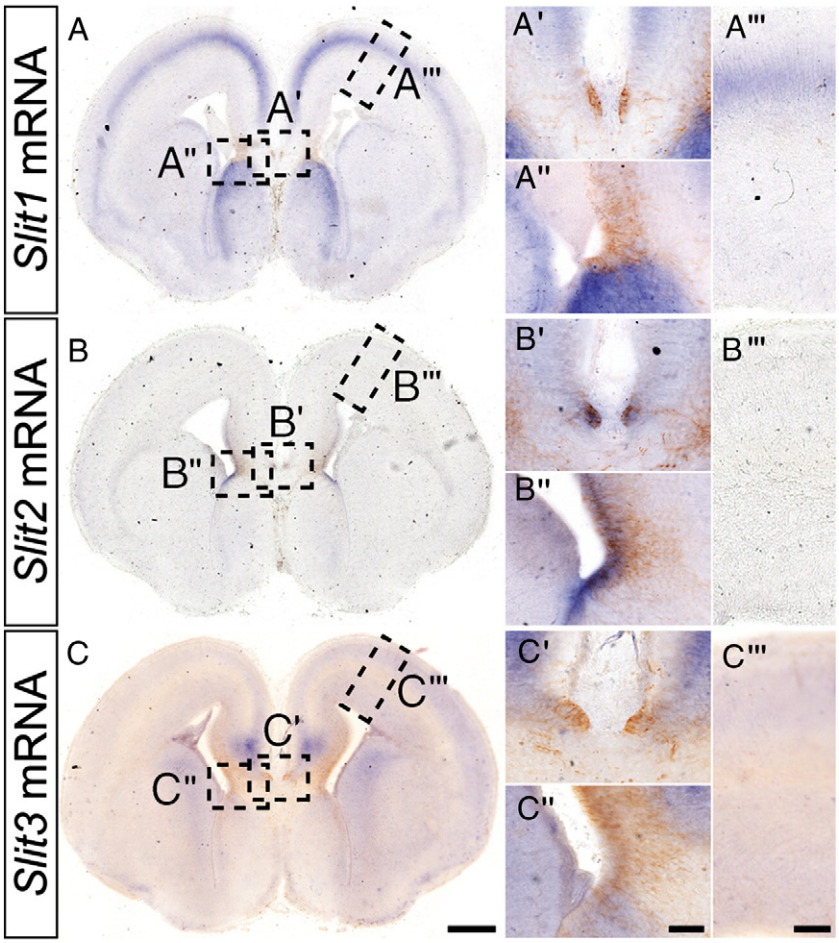

Fig. 1. Expression of *Slit1*, *Slit2* and *Slit3* in the cortex and at the telencephalic midline. *In situ* hybridisation for *Slit1* (A–A‴), Slit 2 (B–B‴) and *Slit3* (C–C‴) mRNA (purple precipitate) on coronal brain sections of E16 wildtype mice, followed by anti-GFAP immunohistochemistry (brown precipitate; n = 3 animals assessed for each probe). Of the three Slit family members, *Slit1* was strongly expressed in the cortical plate, particularly in deeper layers (A, A‴) and *Slit3* was expressed at very low levels in the cortical plate (C‴). *Slit1* and *Slit3* were expressed at very low levels in the septum (A, C). Within midline glial populations, *Slit1*, *Slit2* and *Slit3* were expressed in the indusium griseum (A′, B′, C′), but only *Slit2* expression overlapped with GFAP expression, indicating that *Slit2* was expressed in the glia of the indusium griseum. All three *Slits* were expressed in the glial wedge (A′′, B′′ C′′). Sense probes were used as a control and showed no labelling (not shown). Scale bar in C = 500 μm for A, B and C; scale bar in C′′ = 100 μm (A′, B′, C′, A′′, B′′ and C′′); scale bar in C‴ = 100 μm (A‴, B‴, C‴).

callosum (Fig. 4J–L); however this phenotype was only found in 33% (4/12) of knockout embryos between E16 and P0. The remaining knockout embryos exhibited callosal formation that was indistinguishable from that of wildtype littermate controls (data not shown). Heterozygous animals of each *Slit* knockout strain displayed normal callosal development.

Slit1$^{-/-}$; *Slit2*$^{-/-}$ *double mutant mice exhibit callosal agenesis*

The above analysis of single gene knockouts indicated that *Slit2* is the predominant family member involved in corpus callosum formation. However, the role of *Slit1* in callosal development remained unclear, as the loss of *Slit1* expression may have been functionally compensated for by *Slit2*. We hypothesised that if *Slit1* expression was required for callosal development, then removal of both *Slit1* and *Slit2* would culminate in a more severe callosal phenotype than that observed in mice deficient in *Slit2* alone. To test this hypothesis we analysed the brains of *Slit1*$^{-/-}$; *Slit2*$^{-/-}$ mice using GAP43 immunohistochemistry at E17. This experiment was possible because *Slit1*$^{-/-}$ mice survive to adulthood and are fertile, allowing a more thorough dissection of the role of *Slit1* in brain development. Removing one copy of *Slit2* on a *Slit1*$^{-/-}$ knockout background did not affect callosal formation, as no difference was observed between wildtype and *Slit1*$^{-/-}$; *Slit2*$^{+/-}$ mice at the developing cortical midline at E17 (compare Fig. 5A–C with J–L). However, *Slit1*$^{-/-}$; *Slit2*$^{-/-}$ mice exhibited a more severe phenotype than that observed in *Slit2*$^{-/-}$ mice, as agenesis of the corpus callosum was evident in 100% of double knockout mice (Fig. 5M–O). Furthermore, callosal axons appeared to be actively avoiding the midline, instead projecting into the lateral septum. To validate these findings, tract-tracing was performed using the carbocyanine dye, DiI, injected into the neocortex of wildtype or *Slit1*$^{-/-}$; *Slit2*$^{-/-}$ brains at E17. Following dye transport, analysis of coronal sections of the telencephalon demonstrated that no neocortical axons crossed the midline in the *Slit1*$^{-/-}$; *Slit2*$^{-/-}$ brains (Fig. 5P–U). The increased severity of callosal defects in *Slit1*$^{-/-}$; *Slit2*$^{-/-}$ mice compared to *Slit2*$^{-/-}$ mice indicates that both genes are required to regulate the formation of this axon tract.

We next generated both *Slit1*$^{-/-}$; *Slit3*$^{+/-}$ and *Slit1*$^{-/-}$; *Slit3*$^{-/-}$ mice. *Slit1*$^{-/-}$; *Slit3*$^{+/-}$ animals displayed normal callosal development (Fig. 5D–F), as did 58% of the *Slit1*$^{-/-}$; *Slit3*$^{-/-}$ mice (Fig. 5G–I). The other 42% (5/12) of *Slit1*$^{-/-}$; *Slit3*$^{-/-}$ mice exhibited a callosal dysgenesis phenotype similar in penetrance and phenotype to that of *Slit3*$^{-/-}$ mice (Fig. 5G–I). This suggests that *Slit1* and *Slit3* are not synergistic in this context, and regulate callosal formation via different mechanisms, as removing both alleles of *Slit1* in a *Slit3*$^{-/-}$ background did not significantly increase the percentage of embryos with a more severe phenotype than that of *Slit3*$^{-/-}$ mice. Collectively, these data indicate that *Slit2* plays the predominant role in midline commissure formation in the mouse brain, with minor roles played by both *Slit1* and *Slit3*.

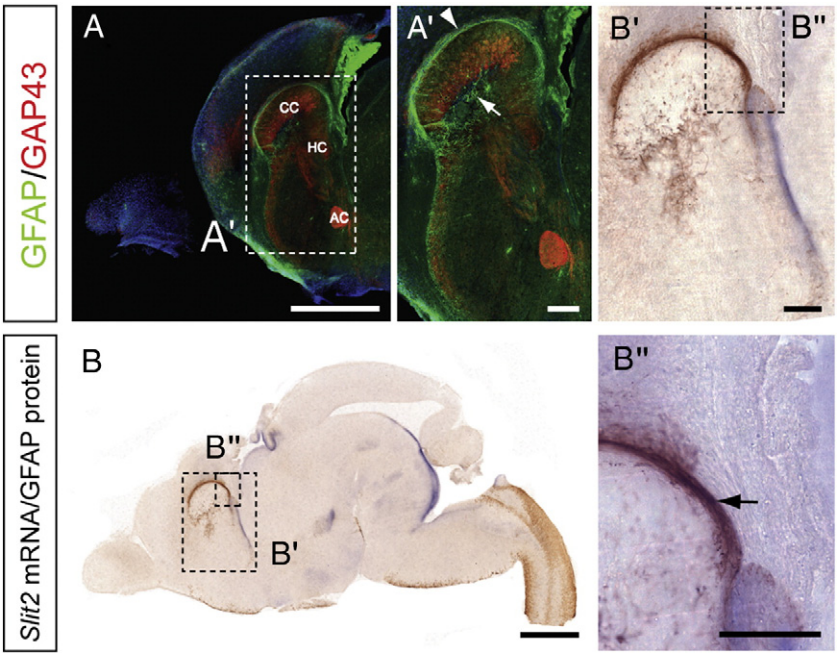

Fig. 2. Sagittal sections reveal the rostro-caudal extent of the indusium griseum glia. Sagittal sections of E17 wildtype brains were processed for double anti-GFAP (green) and anti-GAP-43 (red) immunohistochemistry (A, A′). A midline section revealed the forebrain commissures stained with GAP-43: the corpus callosum (CC), hippocampal commissure (HC) and anterior commissure (AC). Glial populations were associated with each commissure and in particular, the indusium griseum glia were evident above the corpus callosum from rostral to caudal (arrowhead in A′), the glial wedge lies under the rostral part of the corpus callosum (arrow in A′). To examine Slit2 expression in these glia, midline sagittal sections were processed for Slit-2 *in situ* hybridisation (B, B′, B″). Slit2 expression was most evident in the indusium griseum glia in this plane of section (arrow in B″). Scale bars = 1 mm A, B; 200 μm A′, B′, B″.

Some Robo1-positive axons cross the midline in Slit2$^{-/-}$ mice

In *Slit2*$^{-/-}$ mice a significant proportion of axons still crossed the cortical midline within the corpus callosum (Fig. 4G–I). As *Robo1* has been implicated as the predominant *Slit* receptor involved in callosal development (Andrews et al., 2006), we next investigated the expression of Robo1 in *Slit2*$^{-/-}$ mice at E17 to determine if Robo1-expressing axons cross the midline normally in the absence of the *Slit2* ligand. In wildtype mice, Robo1-expressing axons crossed the midline in the dorsal portion of the callosal tract at both rostral and caudal levels (Fig. 6A, C). Likewise, in *Slit2*$^{-/-}$ mice, many Robo1-expressing axons crossed the midline in the dorsal portion of the corpus callosum (Fig. 6B, D). However, some Robo1-expressing axons formed aberrant projections into the septum

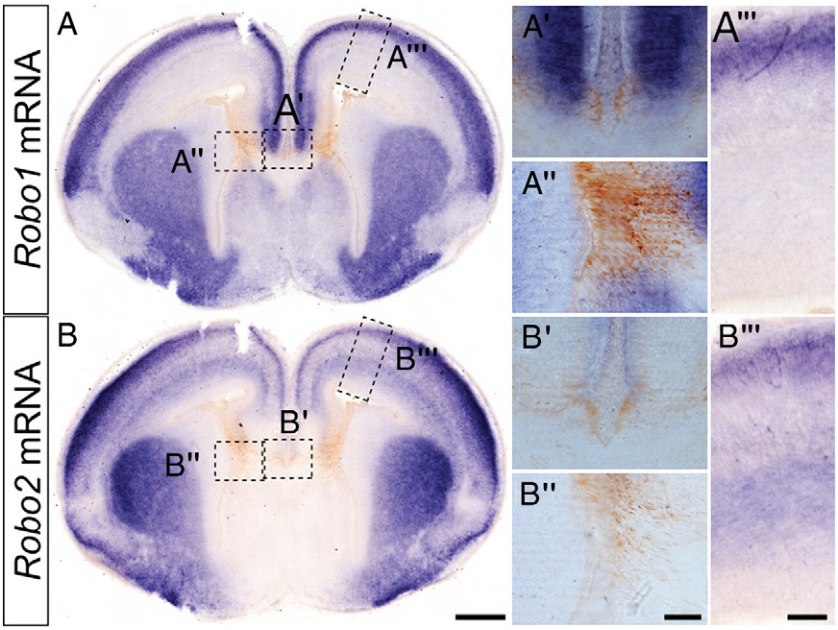

Fig. 3. *Robo1* and *Robo2* expression in the cortex and midline. *In situ* hybridisation probes against *Robo1* (A–A‴) and *Robo2* (B–B‴) were used to analyse their mRNA profiles (purple precipitate) at E16, followed by anti-GFAP immunohistochemistry (brown precipitate; n = 3 animals analysed for each probe). *Robo1* and *Robo2* were expressed in the indusium griseum but their expression did not overlap with GFAP staining (A′, B′). *Robo1* (B″), but not *Robo2* (A″), was expressed in the glial wedge and, as previously shown (Shu and Richards, 2001), both genes were highly expressed in the cortical plate (A‴, B‴). Sense probes were used as a control and showed no specific labelling (not shown). Scale bar in B = 500 μm for A, and B; scale bar in B′′ = 100 μm for panels A′, B′, A′′ and B′′); scale bar in B‴ = 100 μm in A‴ and B‴.

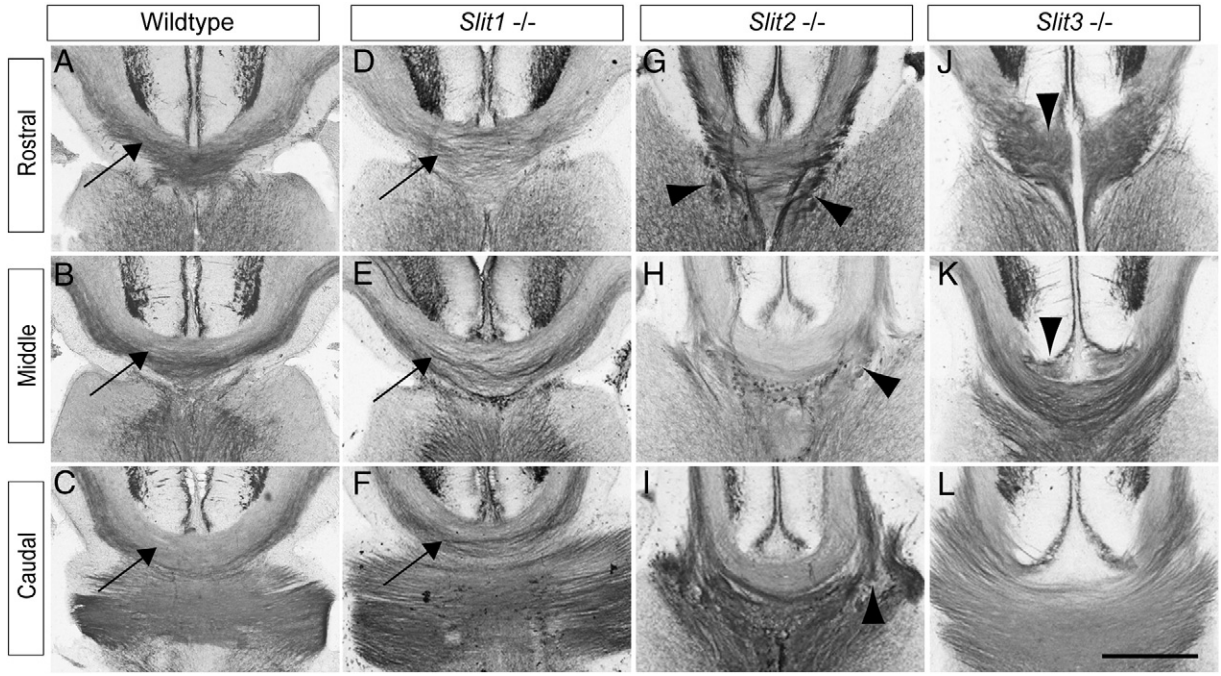

Fig. 4. A comparison of corpus callosum phenotypes in *Slit1*, *Slit2* and *Slit3* mutant mice. Expression of GAP43 at rostral, middle and caudal levels of the cortical midline of E17 wildtype (n = 3) (A–C), *Slit1*$^{-/-}$ (D–F; n = 5), *Slit2*$^{-/-}$ (G–I; n = 5) and *Slit3*$^{-/-}$ (J–L) mice. In both wildtype and *Slit1*$^{-/-}$ mice, callosal axons traversed the cortical midline normally (arrows in A–F). In *Slit2*$^{-/-}$ mice, a subpopulation of callosal axons ectopically entered the septum (arrowheads in G–I). In approximately 30% of *Slit3*$^{-/-}$ mice, axons in the rostral region of the corpus callosum failed to cross the midline (arrowhead in J) and axons in the dorsal portion of the corpus callosum at middle levels were disrupted (arrowhead in K). Scale bar = 300 μm.

(arrowheads in Fig. 6B, D), although whether these axons arose from the corpus callosum or the hippocampal commissure is unknown as both tracts express Robo1 and both are disrupted in *Robo1*$^{-/-}$ mice (Andrews et al., 2006). When considered in light of the strong expression of *Slit1* within the septum, when pioneering axons from the cingulate cortex are first crossing the midline (Koester and O'Leary, 1994; Rash and Richards, 2001), together with the callosal agenesis observed in *Slit1*$^{-/-}$; *Slit2*$^{-/-}$ mice (Fig. 6M–O), these findings suggest that the role of *Slit1* may be to guide Robo1-expressing pioneering axons from the cingulate cortex during the earliest stages of callosal formation.

Slit2-mediated repulsion of neocortical axons is transduced by Robo1

Given that the requirement for Robo1 in callosal axon guidance has not been previously formally tested using an *in vitro* assay, we

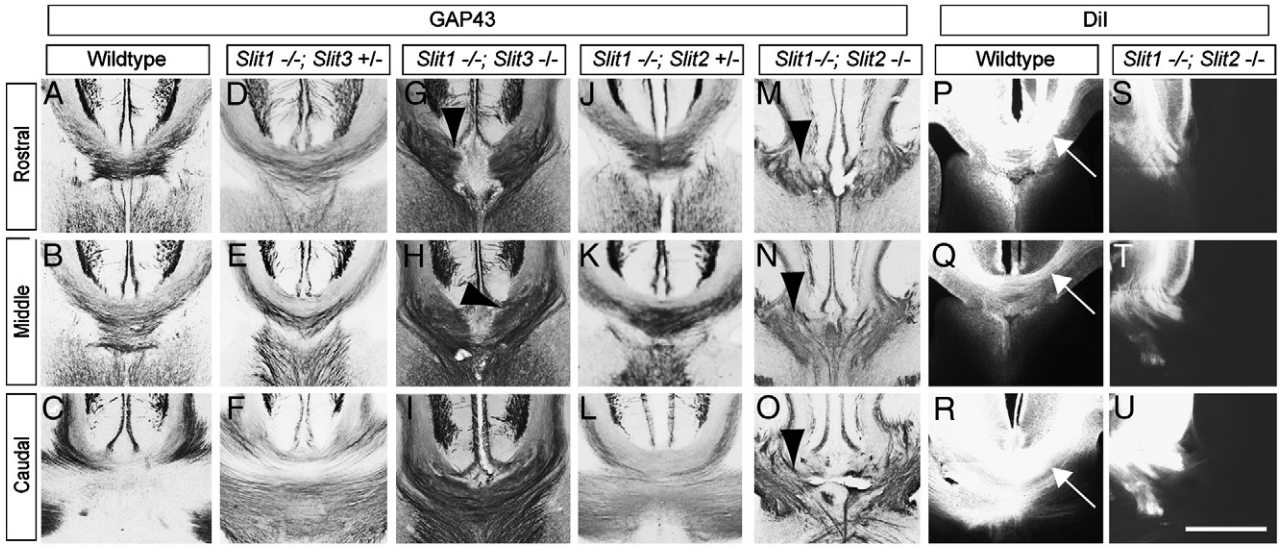

Fig. 5. Comparison of corpus callosum phenotypes in compound *Slit* mutant mice. (A–O) Expression of GAP43 at the cortical midline of E17 wildtype (A–C), *Slit1*$^{-/-}$; *Slit3*$^{+/-}$ (10/14 had no phenotype, the other 4 showed a mild phenotype D–F), *Slit1*$^{-/-}$; *Slit3*$^{-/-}$ (n = 5/12 had this phenotype; 7/12 had no phenotype G–I), *Slit1*$^{-/-}$; *Slit2*$^{+/-}$ (J–L n = 3) and *Slit1*$^{-/-}$; *Slit2*$^{-/-}$ (M–O; n = 6) mice. In wildtype (A–C), *Slit1*$^{-/-}$; *Slit3*$^{+/-}$ (D–F) and *Slit1*$^{-/-}$; *Slit2*$^{+/-}$ (J–L) mice, callosal axons traversed the cortical midline normally. In approximately 40% of *Slit1*$^{-/-}$; *Slit3*$^{-/-}$ mice, axons in the rostral region of the corpus callosum failed to cross the midline (arrowhead in G) and axons in the dorsal portion of the corpus callosum at middle levels were disrupted (arrowhead in H). *Slit1*$^{-/-}$; *Slit2*$^{-/-}$ mice displayed agenesis of the corpus callosum, with axons turning away from the midline (arrowheads in M–O). (P–U) Analysis of corpus callosum formation in wildtype and *Slit1*$^{-/-}$; *Slit2*$^{-/-}$ mice using the carbocyanine dye, DiI, revealed that callosal axons crossed the midline normally in wildtype mice (n = 3) (arrows in P–R). However, no DiI-labelled axons were seen in the contralateral hemisphere of *Slit1*$^{-/-}$; *Slit2*$^{-/-}$ mice (n = 3) (S–U), indicative of callosal agenesis in this strain. Scale bar = 300 μm.

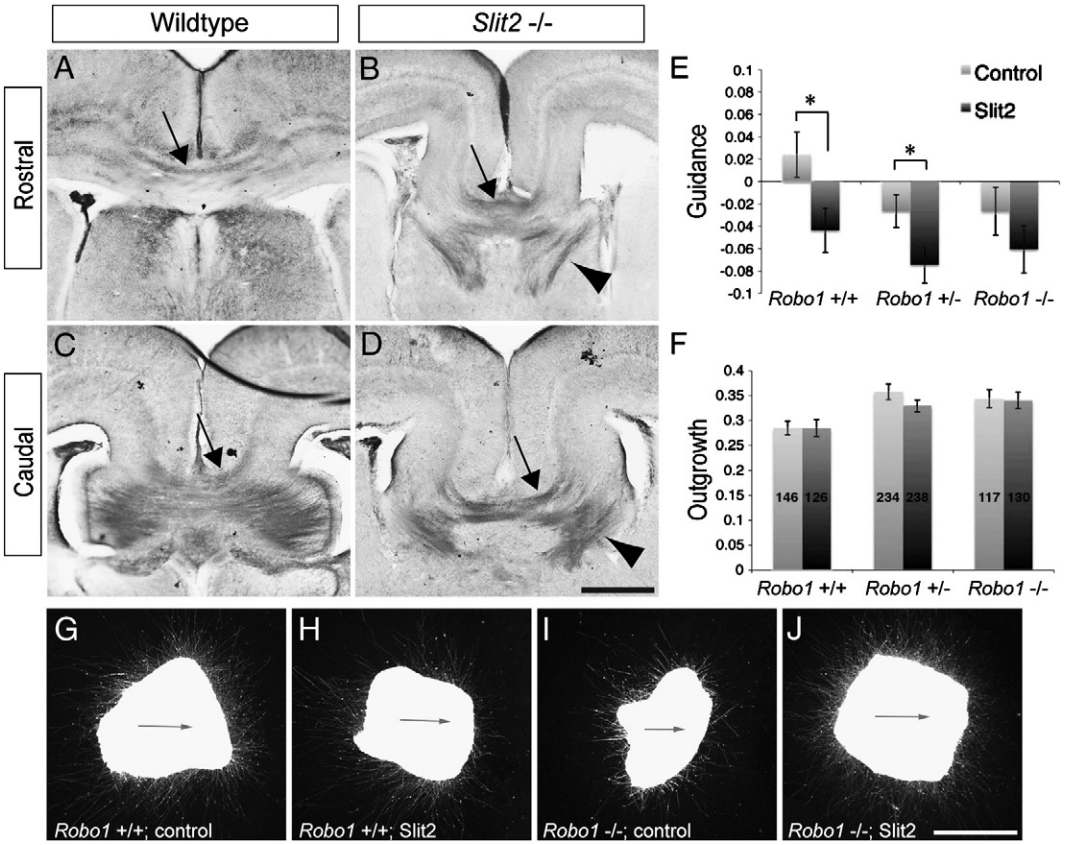

Fig. 6. Slit2 and Robo1 interactions at the cortical midline. Expression of Robo1 at rostral and caudal levels of the cortical midline in E17 wildtype (A, C) and *Slit2*$^{-/-}$ (B, D) mice (n = 3). In wildtype mice, Robo1-expressing axons were located in the dorsal region of the corpus callosum (arrows in A, C). In *Slit2*$^{-/-}$ mice, some Robo1-expressing axons were observed crossing in the dorsal region of the corpus callosum (arrows in B, D), suggestive of axons derived from the cingulate cortex. Another subpopulation of Robo1-expressing axons was observed projecting into the septum (arrowheads in B, D) suggesting that these axons require both Robo1 and Slit2 for pre-crossing callosal guidance. To test this hypothesis, neocortical explants from E17 *Robo1*$^{+/+}$; *Robo1*$^{+/-}$ and *Robo1*$^{-/-}$ mice were paired with Slit2-expressing cell blocks (G–J; arrow indicates the direction of the cell block). As previously shown, neocortical axons from wildtype mice were significantly repelled by Slit2, whereas axons from *Robo1*$^{-/-}$ mice showed no significant difference from controls (E). No significant difference was observed in the outgrowth of axons from explants derived from tissue of any genotype (F). The number of explants per condition is shown inside the bars for outgrowth in F. The same explants were analysed for guidance and outgrowth. Scale bar in D = 200 μm for A–D. Scale bar in J = 200 μm for G–J.

used *Robo1*$^{-/-}$ mice in an explant co-culture experiment to examine Slit2-mediated repulsion. E17 neocortical explants from *Robo1*$^{-/-}$, *Robo1*$^{+/-}$ and *Robo1*$^{+/+}$ littermates were dissected and cultured next to Slit2-expressing or control cell blocks for two days in a semi-dry collagen matrix (Fig. 6G–J). Whereas axons from E17 *Robo1*$^{+/+}$ and *Robo1*$^{+/-}$ neocortical tissue were repelled by Slit2 in comparison to explants cultured next to control cell blocks (Fig. 6E; $p<0.05$, 2-tailed Student's *t*-test), there was no significant difference between explants from *Robo1*$^{-/-}$ mice cultured next to Slit2-expressing or control cell blocks (Fig. 6E; $p>0.05$ 2-tailed Student's *t*-test). No significant changes in outgrowth were observed between the conditions for any of the genotypes (Fig. 6F; $p>0.05$, 2-tailed Student's *t*-test). This result, together with the fact that *Robo1*, but not *Robo2* single mutants display callosal axon guidance defects (Andrews et al., 2006), suggests that Robo1 is the major receptor that neocortical callosal axons use to transduce the Slit2 signal in pre-midline-crossing axons.

Axon guidance defects in post-crossing callosal axons are seen in Slit2$^{-/-}$ *but not Robo1*$^{-/-}$ *mice*

Collectively, the *in vitro* data presented above, and the reported phenotypes of *Slit2*$^{-/-}$ and *Robo1*$^{-/-}$ mice (Andrews et al., 2006; Bagri et al., 2002), as well as the aberrant projection of Robo1-expressing axons into the septum of *Slit2*$^{-/-}$ mice, suggest that *Slit2* and *Robo1* are central to callosal formation. However, whether *Robo1* is the only receptor for the *Slit* ligands in this developmental context remains undefined. Our previous analysis of the *Robo1*$^{-/-}$ phenotype indicated that, as in *Slit2*$^{-/-}$ mice, some callosal axons crossed the midline (Andrews et al., 2006). For *Slit2*$^{-/-}$ mice we have further shown that this ligand guides both pre-crossing and post-crossing callosal axons (Shu et al., 2003c). We therefore hypothesised that if *Robo1* is sufficient for *Slit2* signalling in this system then *Robo1*$^{-/-}$ mice should phenocopy *Slit2*$^{-/-}$ mice. To investigate this we examined callosal tract formation in *Slit2*$^{-/-}$ and *Robo1*$^{-/-}$ mice at E17 using diffusion magnetic resonance imaging (dMRI), followed by computer-assisted tractography.

Diffusion MRI tractography is based on water diffusion measured by MRI, where the axonal membrane acts as a diffusion constraint. This anisotropic diffusion of water molecules along axon tracts allows for three-dimensional streamlines to be propagated along these pathways and the parameters used for this analysis have previously been established and verified for the mouse brain (Moldrich et al., 2010; Ren et al., 2007). Using this approach, the trajectory of callosal axons was mapped in *Slit2*$^{-/-}$ and *Robo1*$^{-/-}$ mice compared to wildtype littermates.

In wildtype mice, the callosal axons that cross the midline rostrally (rostrum) predominantly originate from the rostral neocortex and project to their homotypic target in the contralateral hemisphere (Ozaki and Wahlsten, 1992). Similarly, callosal axons that cross the midline in the middle (body) and caudal (splenium) regions project to the middle and caudal areas of the cortex, respectively (Ozaki and Wahlsten, 1992). This phenotype was recapitulated using dMRI and tractography of control embryos at E17. A ROI (region of interest)

was placed near the cortical midline of the left hemisphere encompassing the rostral, middle and caudal cortical regions, and the streamlines arising from these regions were pseudo-coloured with yellow (motor cortex), red (parietal cortex) and blue (visual cortex) respectively (Fig. 7). Streamlines, which are representative of axon tracts, were generated from these cortical ROIs. In wildtype mice, callosal streamlines from all regions of the cortex crossed the midline in a rostro-caudal topography as previously shown (Ozaki and Wahlsten, 1992; Ren et al., 2007) and did not enter the septum. However, in *Slit2*$^{-/-}$ and *Robo1*$^{-/-}$ mice, a population of callosal streamlines failed to cross the midline and entered the septum in the ipsilateral hemisphere (arrowheads in Fig. 7B, C), reflecting our immunohistochemical findings (Fig. 4; see also Andrews et al., 2006). In both *Robo1*$^{-/-}$ and *Slit2*$^{-/-}$ mice, the ectopic callosal axon tracts that entered the septum arose from either the rostral (yellow) or caudal (red) regions of the cortex (Fig. 7B, C).

To examine the origin and trajectory of the tracts that crossed the midline in *Slit2*$^{-/-}$ and *Robo1*$^{-/-}$ mice, we traced their projections into the contralateral hemisphere (Fig. 7D–F). In wildtype animals, streamlines that crossed the midline turned dorsally to enter the contralateral hemisphere (Fig. 7D). In *Slit2*$^{-/-}$ mice, however, some post-crossing callosal streamlines aberrantly entered the septum of the contralateral hemisphere, supporting previous evidence that *Slit2* is required for the guidance of post-crossing commissural axons *in vivo* (Shu et al., 2003c). This aberrant population of post-crossing streamlines in *Slit2*$^{-/-}$ mice arose from ROIs in the rostral and parietal cortices (Fig. 7E). In contrast, streamlines crossing the midline in *Robo1*$^{-/-}$ mice displayed a normal contralateral trajectory, innervating their homotopic region within the contralateral hemisphere (Fig. 7F). These data indicate that *Slit2*$^{-/-}$ and *Robo1*$^{-/-}$ mice have similar but distinct phenotypes, particularly in regard to the guidance of post-crossing axons, and suggest the involvement of additional receptors in this process.

An additional phenotype previously observed in the *Robo1*$^{-/-}$ mice involved axons from the hippocampal commissure intermingling with axons from the corpus callosum (Andrews et al., 2006), indicating a potential role for *Robo1* in maintaining the separation of these two commissural axon tracts during normal development. In order to compare the development of the hippocampal commissure axons in *Robo1*$^{-/-}$ and *Slit2*$^{-/-}$ mice, ROIs were placed in the corpus callosum (at rostral, middle and caudal levels) and at the caudal midline region of the cortex below the genu of the corpus callosum, where the hippocampal commissural axons cross the midline (Fig. 8). Consistent with previous reports (Andrews et al., 2006), the tractography streamlines of the hippocampal commissure intermingled with the callosal streamlines in the *Robo1*$^{-/-}$ mice

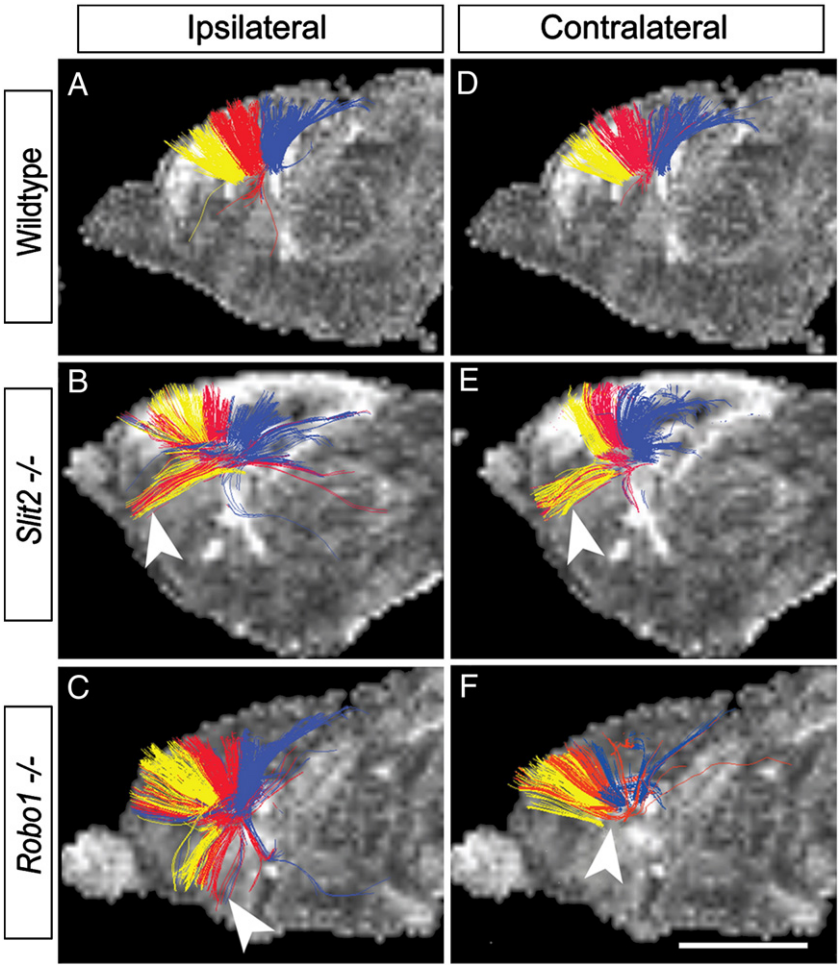

Fig. 7. dMRI and tractography in *Slit2*$^{-/-}$ and *Robo1*$^{-/-}$ brains. Diffusion MRI and tractography was performed on E17 brains from wildtype (A, D; n = 3), *Slit2*$^{-/-}$ (B, E; n = 3) and *Robo1*$^{-/-}$ (C, F; n = 3) mice. Tractography streamlines represent axonal tracts traced from ROIs placed in the left hemisphere, near the cortical midline at rostral, middle and caudal levels. The tracts arising from these regions were pseudo-coloured with yellow (motor cortex), red (parietal cortex) and blue (visual cortex), respectively. In wildtype mice, axonal tracts from rostral, middle, and caudal areas in the ipsilateral hemisphere (A) projected to homotopic regions in the contralateral hemisphere (B). In *Slit2*$^{-/-}$ mice, some pre-crossing callosal axon tracts ectopically projected into rostral and ventral regions of the brain (arrowhead in B). In the contralateral hemisphere, post-crossing callosal axon tracts also projected ectopically into rostral and ventral regions (arrowhead in E). These ectopic axon tracts appeared to arise from motor and parietal areas, whereas axon tracts from visual areas were not affected (B, E). In *Robo1*$^{-/-}$ mice, pre-crossing callosal axon tracts projected ectopically into ventral regions (arrowhead in C). In the contralateral hemisphere, post-crossing callosal axon tracts projected relatively normally (arrow in F). Scale bar = 500 μm.

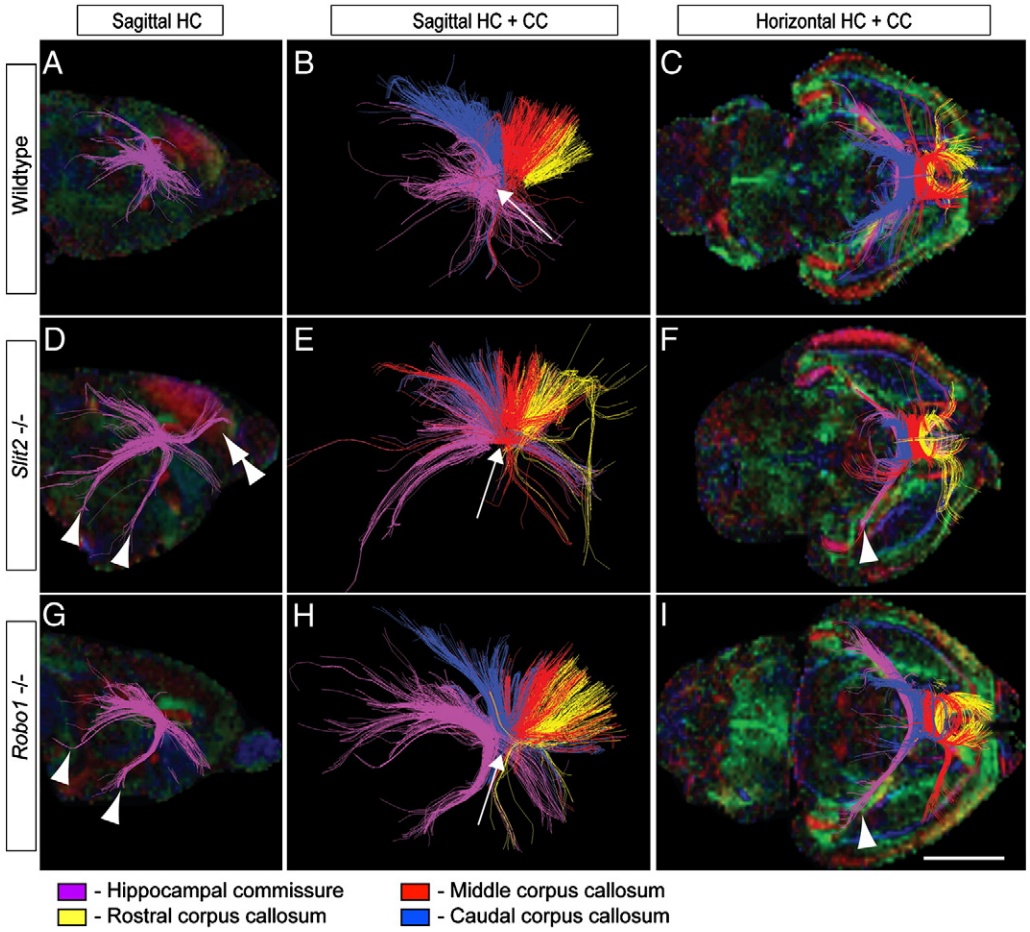

Fig. 8. dMRI and tractography of axons from both the corpus callosum and the hippocampal commissure in *Slit2*$^{-/-}$ and *Robo1*$^{-/-}$ brains. E17 wildtype (A–C), *Slit2*$^{-/-}$ (D–F) and *Robo1*$^{-/-}$ (G–I) brains (n = 3 for each) were scanned for diffusion MRI and subsequent tractography. ROIs were placed in the rostral (yellow), middle (red) and caudal (blue) regions of the corpus callosum, as well as within the hippocampal commissure (purple). Tracts were then analysed in both the sagittal (A, B, D, E, G, H) and horizontal (C, F, I) planes. In panels A, D and G only the hippocampal tracts are shown in the context of the fractional anisotropy image of the brain, whereas in the remaining panels the hippocampal tracts are shown in relation to the callosal tracts. The analysis revealed ectopic hippocampal projections from the fornix in both *Slit2*$^{-/-}$ and *Robo1*$^{-/-}$ mutant strains. These tracts projected further rostrally, ventrally and laterally (arrowheads in D–I) in both mutant strains compared to wildtypes (A–C). Furthermore, some hippocampal axon tracts in *Slit2*$^{-/-}$ mice aberrantly projected towards the olfactory bulb (double arrowhead in D). In sagittal view it is evident that the axon tracts of both the corpus callosum and hippocampal commissure came into close apposition but did not intermingle in wildtype brains (arrow in C). However in both *Slit2*$^{-/-}$ and *Robo1*$^{-/-}$ brains the hippocampal commissure tracts projected ectopically too far rostrally through the corpus callosum, thus intermingling with the callosal tracts at the midline (arrow in E, H). In images A, D, E and C, F, I, streamlines overlay the horizontal plane of a colour-coded fractional anisotropy image whereby the colours indicate oriented tissue as follows: red, mediolateral; blue, dorsoventral; green, rostrocaudal. HC = hippocampal commissure; CC = corpus callosum. Scale bar = 700 μm A, D, G; 400 μm B, C, E, F, H, I.

(Fig. 8G–I). A similar phenotype was also observed in the *Slit2*$^{-/-}$ mice, in which the streamlines from the hippocampal commissure intermingled with the rostral and caudal callosal streamlines (Fig. 8D–F). The hippocampal commissure streamlines in *Robo1*$^{-/-}$ and *Slit2*$^{-/-}$ mice also overshot their targets and extended further caudally than in the wildtype animals (Fig. 8C, F, I). An aberrant population of hippocampal commissure tracts was also observed projecting rostrally in the *Slit2*$^{-/-}$ mice, a phenotype not observed in the *Robo1*$^{-/-}$ mutants.

The corpus callosum is ventrally displaced in Slit2 mutant mice

During our analysis of the *Slit2*$^{-/-}$ mutant mice we observed that the corpus callosum appeared ventrally displaced when compared to that of wildtype mice. To quantify this observation, the distance from the pial surface to the dorsal edge of the corpus callosum was measured in coronal sections of wildtype and *Slit2*$^{-/-}$ brains at E17. To control for potential differences in brain size between wildtype and *Slit2*$^{-/-}$ mice, each measurement was divided by the total dorso-ventral height of the respective brain. Statistical analyses showed that callosal axons in *Slit2*$^{-/-}$ mice crossed the midline significantly further ventrally than in the wildtype mice at all levels of the corpus callosum examined (Fig. 9K).

Slit mutant and Robo1$^{-/-}$ *mice display defects in midline glial development*

Studies in zebrafish have shown that *Slit* is required for the correct positioning of forebrain glial populations during development (Barresi et al., 2005). Furthermore, as *Slit2*$^{-/-}$ mice showed a ventral displacement of the corpus callosum, we next sought to determine if this phenotype might be due to disruptions in midline glial development in these mice. To examine this we utilised two markers of glial cells, the astrocytic marker GFAP (Bignami and Dahl, 1974), and the astroglial marker, astrocyte glutamate transporter (GLAST) (Hartfuss et al., 2001). As previously shown (Shu et al., 2003b), in wildtype mice at E17 the indusium griseum glia differentiate above the corpus callosum (arrowhead in Fig. 9A), and the glial wedge develops lateral and ventral to the corpus callosum (arrow in Fig. 9A). No difference in glial positioning was observed in *Slit1*$^{-/-}$ or *Slit1*$^{-/-}$; *Slit2*$^{+/-}$ mice (Fig. 9C, D, G, H). Moreover, the position of the glial wedge remained relatively stable on the different mutant backgrounds with respect to dorso-ventral position. However, in both *Slit2*$^{-/-}$ mice and *Slit1*$^{-/-}$;

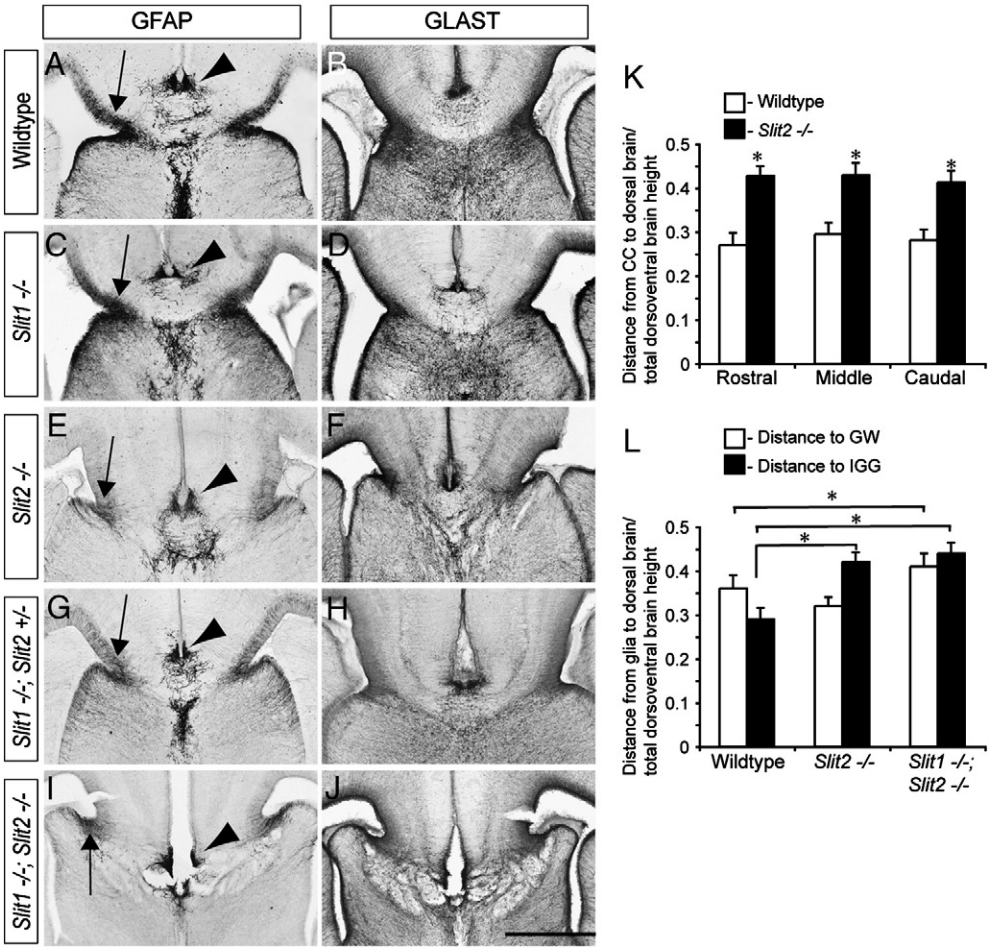

Fig. 9. *Slit1* and *Slit2* regulate the dorso-ventral position of the glial wedge and the indusium griseum glia. Coronal sections through the telencephalon of E17 wildtype (A, B; n = 2), *Slit1*$^{-/-}$ (C, D; n = 5), *Slit2*$^{-/-}$ (E, F; n = 5), *Slit1*$^{-/-}$; *Slit2*$^{+/-}$ (G, H; n = 3) and *Slit1*$^{-/-}$; *Slit2*$^{-/-}$ (I, J; n = 6), showing GFAP (A, C, E, G, I) and GLAST (B, D, F, H, J) immunohistochemistry. The indusium griseum glia (arrowhead in A, C, G) differentiated above the corpus callosum, whereas the glial wedge (arrow in A, C, G) developed below the corpus callosum in wildtype, *Slit1*$^{-/-}$ and *Slit1*$^{-/-}$; *Slit/2*$^{+/-}$ brains. In *Slit2*$^{-/-}$ and *Slit1*$^{-/-}$; *Slit/2*$^{-/-}$ brains the indusium griseum glia (arrowheads in E and I, respectively) were shifted ventrally with respect to the glial wedge (arrows in E and I, respectively). Similar phenotypes were verified using GLAST labelling in all genotypes. (K) Quantification showed that the corpus callosum was ventrally displaced in *Slit2*$^{-/-}$ mice at rostral, middle and caudal levels. (L) The indusium griseum glia were ventrally displaced in both *Slit2*$^{-/-}$ and *Slit1*$^{-/-}$; *Slit/2*$^{-/-}$ brains, and the glial wedge was ventrally displaced in *Slit1*$^{-/-}$; *Slit/2*$^{-/-}$ brains. Scale bar = 200 μm for all panels.

Slit2$^{-/-}$ mice the indusium griseum glia were displaced ventrally (Fig. 9E, F, I, J, L). In *Slit2*$^{-/-}$ mice, the indusium griseum glia were located at a similar dorso-ventral position to the glial wedge, whereas in *Slit1*$^{-/-}$; *Slit2*$^{-/-}$ mice they were located below the glial wedge. Given that callosal axons approach and cross the midline between these two glial populations, the mispositioning of these glia in *Slit2*$^{-/-}$ and *Slit1*$^{-/-}$; *Slit2*$^{-/-}$ mice suggests that glial abnormalities may in part underlie the callosal phenotypes exhibited by these mice.

To examine the development of this phenotype, we performed GFAP staining in *Slit2*$^{-/-}$ and *Slit1*$^{-/-}$; *Slit2*$^{-/-}$ mice at E15 and E16 (Fig. 10). The glial wedge begins to develop at E13, but the indusium griseum glia only arise at a later time-point. At both E15 (Fig. 10A–C) and E16 (Fig. 10D–F) the glial wedge appeared normal (arrowheads in Fig. 10) and the indusium griseum glia were not present at either of these stages in *Slit2*$^{-/-}$ and *Slit1*$^{-/-}$; *Slit2*$^{-/-}$ mice or their wildtype littermates. GAP43 staining of axons at E16 (Fig. 10G–H) demonstrated that these axons approached the midline and were beginning to cross the midline in wildtype animals, whereas callosal axons in *Slit2*$^{-/-}$ and *Slit1*$^{-/-}$; *Slit2*$^{-/-}$ mice remained more lateral (arrows in Fig. 10). These data indicate that the phenotype observed at E17 is not likely to be due to abberant glial wedge formation, but rather is coincident with the formation of the indusium griseum glia in these mice.

We next examined whether midline glial populations were disrupted in *Robo1*$^{-/-}$ mice. Double labelling of E17 brains for GAP43 and GFAP revealed that, as with *Slit2*$^{-/-}$ mice, *Robo1*$^{-/-}$ mice displayed ventral displacement of the indusium griseum glia (Fig. 11; results from *Slit1*$^{-/-}$; *Slit2*$^{-/-}$ mice are shown for comparison). When we performed a similar quantification of the distance from the dorsal cortex to the glial wedge and the indusium griseum glia, our analysis revealed that there was no significant increase in the distance to the glial wedge (ratio of wildtype distance to the glial wedge over dorso-ventral brain height 0.357 ± 0.029 (standard deviation for all measurements); ratio of *Robo1*$^{-/-}$ distance to the glial wedge over dorso-ventral brain height 0.387 ± 0.012) but that the indusium griseum glia were significantly displaced ventrally (ratio of wildtype distance to indusium griseum glia over dorso-ventral brain height 0.29 ± 0.026; ratio of *Robo1*$^{-/-}$ distance to indusium griseum glia over dorso-ventral brain height 0.37 ± 0.005; $p < 0.05$, Students *t*-test).

Finally, analysis of GFAP expression in *Slit3*$^{-/-}$ mice did not reveal any defects with respect to the positioning of cortical midline glial populations (Fig. 12). However, the development of the indusium griseum glia appeared abnormal in a number of *Slit3*$^{-/-}$ mice (Fig. 12; 33% penetrant) that also displayed rostral dysgenesis of the corpus callosum. During normal development, the glial cells that comprise the indusium griseum glia arise from the ventricular zone and migrate to the pial surface where they retract their radial process and differentiate into mature glia (Smith et al., 2006). In *Slit3*$^{-/-}$ mice, this second maturational step did not occur in all animals, and the

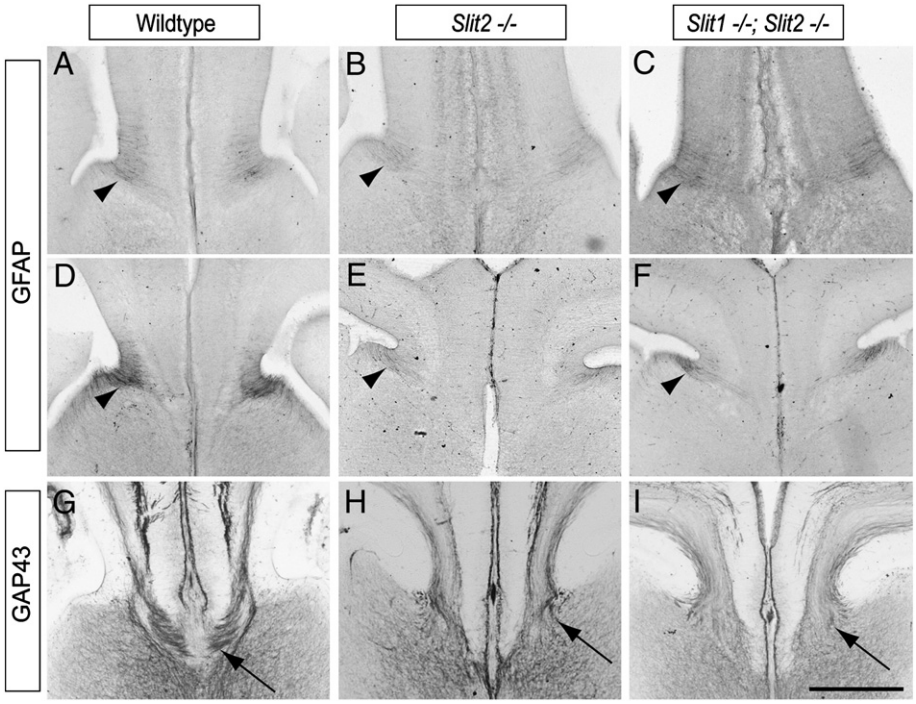

Fig. 10. Midline glial populations appear normal at earlier stages. Coronal sections of E15 (A–C) and E16 (D–1) wildtype (A, D, G), *Slit2*$^{-/-}$ (B, E, H), and *Slit1*$^{-/-}$; *Slit2*$^{-/-}$ (C, F, I) brains were stained with anti-GFAP (A–F) or anti-GAP43 (G–I) antibodies. At E15, the glial wedge is the first midline glial structure to develop and no difference in midline glial development was observed in either mutant strain (A–F; arrowheads). At E16, GAP43-stained axons began to approach the midline in wildtype littermate brains (G; arrow) but remained more lateral in *Slit2*$^{-/-}$ (H; arrow), and *Slit1*$^{-/-}$; *Slit2*$^{-/-}$ (I; arrow) sections. Scale bar in I = 200 μm for all panels.

indusium griseum glia remained underdeveloped, with their glial fibres failing to retract from the ventricular zone (compare Fig. 12A, C, E with B, D, F). Given the expression of *Slit3* in the indusium griseum (in GFAP-negative cells; Fig. 1C) and the different callosal phenotype of *Slit3*$^{-/-}$ mice when compared to other *Slit* mutants (Fig. 3), these data suggest that *Slit3* may act predominantly via the regulation of glial maturation in a non cell-autonomous manner during corpus callosum development.

Discussion

The formation of commissural projections requires a variety of processes to be coordinated in a precise spatiotemporal manner. The development of the largest commissure in the brain, the corpus callosum, provides a salient example of this. For this axon tract to form, callosally projecting neurons must be specified correctly within the cortical germinal zones, and must extend an axon towards the cortical midline. At the midline, the fusion of the telencephalic hemispheres must occur to provide a substrate through which the callosal axons can cross the midline, and glial populations such as the glial wedge and the indusium griseum need to develop in order to specify morphological boundaries and to express critical axon guidance cues (Gobius and Richards, 2011; Lindwall et al., 2007; Piper et al., 2007). Although *Slit2* has previously been identified as an important guidance cue for callosal axons (Bagri et al., 2002; Shu et al., 2003c), this study reveals a much broader role for the Slit family of guidance cues in callosal development than previously recognised, demonstrating that these ligands are required both to guide callosal axons and to regulate the positioning and maturation of glial populations at the cortical midline.

In vivo, down-regulation of *Slit2* at the midline has shown that this ligand regulates the guidance of both pre-crossing and post-crossing callosal axons (Shu et al., 2003c). Furthermore, *Slit2*$^{-/-}$ mice have been reported to display callosal dysgenesis (Bagri et al., 2002). Our data support these findings, with immunohistochemical analyses revealing callosal abnormalities in these mice (Fig. 4), and dMRI demonstrating that populations of pre-crossing and post-crossing callosal axons inappropriately invade the septum in mice lacking

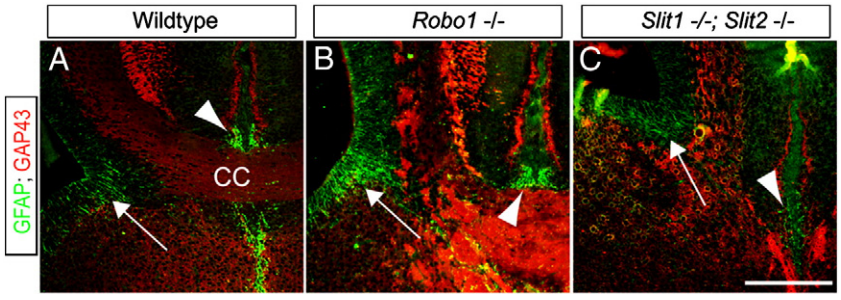

Fig. 11. The indusium griseum is ventrally misplaced in *Robo1*$^{-/-}$ mice. Coronal sections of wildtype (A), *Slit2*$^{-/-}$ (B), *Robo1*$^{-/-}$ (C), and *Slit1*$^{-/-}$; *Slit/2*$^{-/-}$ (D) brains at E17 (n = 3 for each strain and genotype) were analysed for the expression of GFAP (green) and GAP43 (red) to label glia and axons, respectively. In wildtype animals, the indusium griseum glia (arrowheads in all panels) were located dorsal to the corpus callosum (labelled CC in A), whereas the glial wedge (arrows in all panels) was located ventral and lateral to the corpus callosum. The indusium griseum glia were ventrally displaced in both *Slit2*$^{-/-}$ (B) and *Robo1*$^{-/-}$ (C) mice when compared to wildtype animals (A), with *Slit1*$^{-/-}$;*Slit/2*$^{-/-}$ mice displaying an even more severe phenotype (D). Scale bar = 50 μm.

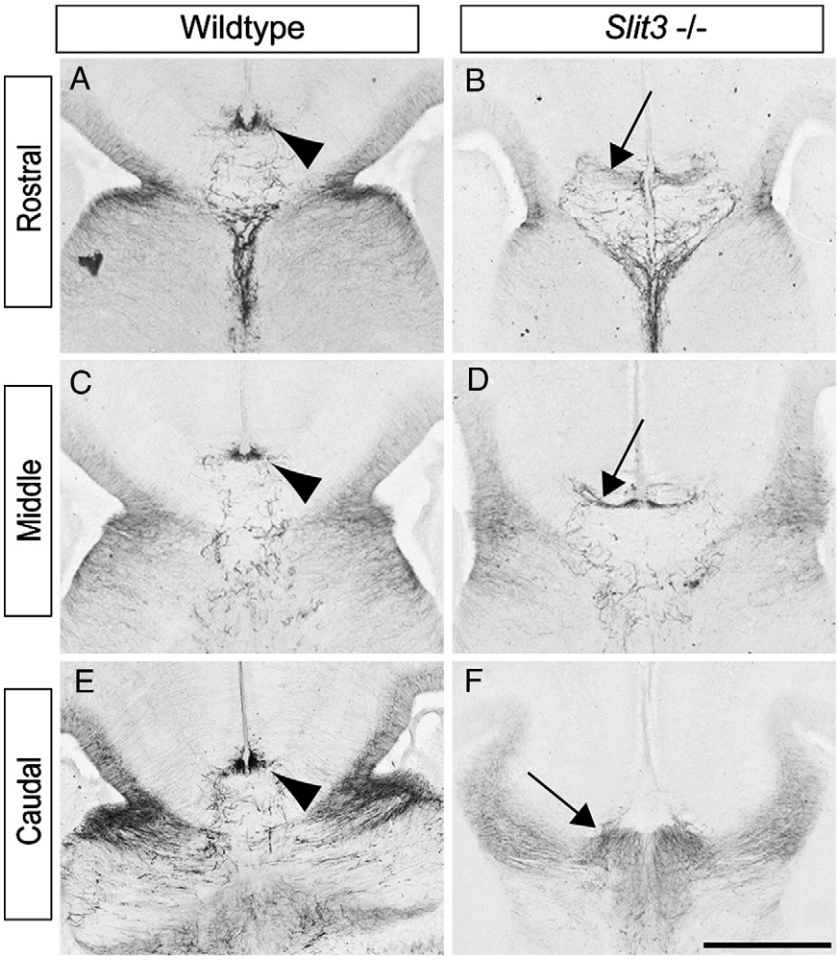

Fig. 12. The indusium griseum glia fail to develop normally in a subset of *Slit3*$^{-/-}$ mice. Expression of GFAP at the cortical midline of E17 wildtype (A, C, E; n = 10) and *Slit3*$^{-/-}$ (B, D, F; n = 10) mice. In wildtype mice, the indusium griseum glia developed above the corpus callosum (arrowheads in A, C, E). In approximately 30% of *Slit3*$^{-/-}$ mice, however, the indusium griseum glia retained their GFAP-positive radial process and failed to fully differentiate (arrows in B, D, F). Scale bar = 200 μm.

the *Slit2* ligand (Figs. 4, 7). Importantly, whereas *Slit1*$^{-/-}$ mice exhibited normal callosal development, *Slit*$^{-/-}$*; Slit2*$^{-/-}$ mice displayed agenesis (complete absence) of the corpus callosum, a phenotype much more severe than that produced in the absence of *Slit2* alone. This is indicative of a synergistic role for *Slit1* in callosal development, but also implies that *Slit2* can compensate for *Slit1* function in *Slit1*$^{-/-}$ mice. Moreover, since some Robo1-positive axons still cross the midline in *Slit2*$^{-/-}$ animals, these data suggest that it is these axons that possibly originate in the cingulate cortex which may be responsive to Slit1. In addition, *Slit3*$^{-/-}$ mice displayed midline commissural deficits, albeit at a reduced penetrance. Collectively, these findings suggest that *Slit2* is the major Slit ligand involved in callosal development, while at the same time demonstrating that *Slit1* and *Slit3* can also contribute to this process.

Previous work by our laboratory and others has shown that *Slit2*$^{-/-}$ mice and *Robo1*$^{-/-}$ or *Robo1*$^{-/-}$*; Robo2*$^{-/-}$ mice display dysgenesis of the corpus callosum (Andrews et al., 2006; Bagri et al., 2002; Lopez-Bendito et al., 2007). In both *Slit2*$^{-/-}$ and *Robo1*$^{-/-}$ mutants, a subpopulation of callosal axons fails to cross the midline, instead coursing aberrantly into the septum (Andrews et al., 2006; Bagri et al., 2002). One conclusion that can be drawn from this is that callosal axons display differential responses to midline guidance cues. Moreover, the similar phenotypes of *Slit2*$^{-/-}$ mice and *Robo1*$^{-/-}$ mice suggested that *Robo1* was sufficient to control all *Slit2*-mediated guidance at the cortical midline. However, our dMRI analyses (Fig. 7) refute this conclusion, demonstrating that, whereas post-crossing callosal axons target the contralateral hemisphere normally in *Robo1*$^{-/-}$ mice, a subpopulation of post-crossing callosal axons is misguided in *Slit2*$^{-/-}$ mice. From this we infer that *Slit2*-mediated guidance of post-crossing callosal axons is independent of *Robo1*. Furthermore, a significant proportion of callosal axons still cross the midline in both *Robo1*$^{-/-}$ mice and in *Robo1*$^{-/-}$*; Robo2*$^{-/-}$ mice (Lopez-Bendito et al., 2007), indicative of an additional receptor contributing to *Slit1/2*-mediated guidance of pre-crossing callosal axons. The identity of this receptor is as yet unknown, but a recent report has also hypothesised that additional receptor(s) may be required to mediate Slit-based repulsion in the developing spinal cord (Jaworski et al., 2010), suggesting that other receptors for the Slit ligands await identification.

Previously, we found that axons behave differently across different segments of the corpus callosum in *Netrin1*$^{-/-}$ and deleted in colorectal carcinoma (*DCC*)$^{-/-}$ mice (Ren et al., 2007). Using carbocyanine dye tracing and immunohistochemistry we showed how dMRI tractography could be successfully used to trace axon tracts. In *Netrin1*$^{-/-}$ and *DCC*$^{-/-}$ mice, callosal axons continued to grow and formed Probst bundles where the axons projected rostrocaudally rather than crossing the midline or projecting ventrally into the septum, as seen here in *Robo1*$^{-/-}$ mice. However, the *Netrin1*$^{-/-}$ and *DCC*$^{-/-}$ mice display more severe callosal agenesis than the *Slit2*$^{-/-}$ and *Robo1*$^{-/-}$ mice, where no axons cross the midline, and all forebrain commissures are affected. These results were also demonstrated by the different tractography profiles of these mice and provide further validation of this technique.

Diffusion MRI and tractography in fixed mouse brains has many advantages over dMRI and tractography used in human studies

(Jones and Cercignani, 2010), including high resolution and fewer susceptibility artefacts. Evolution of dMRI modelling from tensor to high angular resolution such as Q-ball has resulted in increased flexibility of the streamline propagation algorithm (Moldrich et al., 2010). However, the dMRI tractography used here is unable to determine how many axons constitute the misprojecting bundles, whether they are afferent or efferent, and from which layer the tracts originate. Unlike carbocyanine dye tracing, dMRI tractography can be seeded from very small ROIs to project tracts, which are ultimately visualised in three dimensions. Such an appreciation of commissural axon tracts allows comparison with multiple tracts from different regions within the same brain (such as the corpus callosum and hippocampal commissure), and allows comparison with different axon guidance mutants (discussed above).

The development of midline glial populations is critical for the formation of the corpus callosum (Piper et al., 2009a; Sánchez-Camacho et al., 2011; Shu et al., 2003a; Smith et al., 2006). Given that Slit has been implicated in glial positioning within the developing zebrafish forebrain (Barresi et al., 2005), we investigated glial development in our *Slit* mutant mice. This analysis revealed significant deficits in the dorso-ventral positioning of midline glial populations, in particular the indusium griseum glia. In both *Slit2*$^{-/-}$ mice and *Slit1*$^{-/-}$; *Slit2*$^{-/-}$ mice, the indusium griseum glia were displaced ventrally relative to the glial wedge and the cortico-septal boundary. Previous work has demonstrated that the glial wedge acts both to prevent callosal axons from entering the septum and to cause them to turn toward the midline (Shu et al., 2003b). Given that the midline is unfused above the indusium griseum, callosal axons must pass ventral to this. Thus, the proper formation of the indusium griseum glia is essential to the development of the corpus callosum. This conclusion is supported by the phenotype of *Fgfr1* conditional knockout mice, which exhibit deficient development of the indusium griseum glia and subsequent callosal agenesis (Smith et al., 2006). The ventral displacement of the indusium griseum glia in *Slit2*$^{-/-}$ and *Slit*$^{-/-}$; *Slit2*$^{-/-}$ mice may place physical constraints on navigating callosal axons. Just how Slit1 and Slit2 regulate positioning of the indusium griseum glia is unclear, but this could occur through the regulation of glial migration from the ventricular surface, or through patterning of this area such that progenitor cells become destined for glial differentiation at certain points along the dorso-ventral axis. BMP7 regulates the development of these same midline glial populations and is also involved in the differentiation and position of both corridor neurons and midline glia (Sánchez-Camacho et al., 2011). Whether BMP7 and Slit-mediated glial development represent independent or interacting molecular mechanisms remains to be determined. Our findings also demonstrate a distinct role for Slit3 in glial maturation, as indusium griseum glia appear less morphologically developed in the absence of this ligand. Our co-labelling studies suggest that Slit2 may act cell-autonomously in indusium griseum glial migration and differentiation but that Slit1 and Slit3 act in a non-cell-autonomous manner.

Another phenotype observed in the *Slit2*$^{-/-}$ and *Slit1*$^{-/-}$; *Slit2*$^{-/-}$ mice was a lack of telencepahlic midline fusion. This process is thought to be mediated by midline zipper glia (Silver et al., 1993). However, neither Robos nor Slits are highly expressed in the pial membrane ventral to the corpus callosum, suggesting that defects in midline fusion may be secondary to a lack of callosal axon crossing or defects in the formation of other midline glial populations. Analysis of earlier developmental stages suggested that midline fusion defects may begin to be apparent as early as E16 in *Slit2*$^{-/-}$ and *Slit1*$^{-/-}$; *Slit2*$^{-/-}$ mice (Fig. 10), but this phenotype was variable between animals.

Finally, previous studies have shown that thalamocortical and corticofugal fibres create an ectopic ventral commissure in *Slit2*$^{-/-}$, *Slit1*$^{-/-}$; *Slit2*$^{-/-}$ and *Robo1*$^{-/-}$; *Robo2*$^{-/-}$ mice (Bagri et al., 2002; Lopez-Bendito et al., 2007). This ectopic ventral commissure, which forms ventral to the anterior commissure and at a similar rostrocaudal level, was also observed in the *Slit1*$^{-/-}$; *Slit2*$^{-/-}$ mice examined here (data not shown). Thus, *Slit1*$^{-/-}$; *Slit2*$^{-/-}$ and *Robo1*$^{-/-}$; *Robo2*$^{-/-}$ mice have very similar defects in other cortical axon tracts, but are not identical with regard to corpus callosum formation. In *Robo1*$^{-/-}$ and *Robo1*$^{-/-}$; *Robo2*$^{-/-}$ mice, some axons still cross the midline via the corpus callosum (Andrews et al., 2006; Lopez-Bendito et al., 2007), whereas in *Slit1*$^{-/-}$; *Slit2*$^{-/-}$ mice no axons cross the midline (Fig. 3). Therefore, the severity of the *Slit1*$^{-/-}$; *Slit2*$^{-/-}$ phenotype is potentially more attributable to glial development defects that could prevent callosal axons from crossing the midline, rather than the classical axon guidance role of these molecules. Further evidence of this is that, *in vitro*, E17 neocortical axons from *Robo1*$^{-/-}$ brains show no significant repulsion by Slit2 compared to controls, demonstrating that Slit2 is sufficient to mediate guidance via Robo1. Hence, the role of Slit1 in this system is likely to involve regulation of the development of the indusium griseum, and possibly the guidance of axons from the cingulate cortex. The severe phenotype of the *Slit1*$^{-/-}$; *Slit2*$^{-/-}$ mice has demonstrated that not only is the generation of the midline glia essential for callosal tract formation, but also that the position of the indusium griseum glia is crucial for the formation of this structure, and that Slits are indispensable for their development.

Methods

Animals

All mice used in this study were bred at The University of Queensland with approval from the institutional Animal Ethics Committee. The wildtype strains used in this study were C57BL/6J and CD1 mice. Timed-pregnant females were obtained by placing male and female mice together overnight. The following day was designated as E0 if the female had a vaginal plug. *Slit1* and *Slit2* mutant mice were obtained from Marc Tessier-Lavigne (Genetech) (Plump et al., 2002) and *Slit3* mutant mice were originally obtained from Marc Tessier-Lavigne with permission from David Ornitz (Washington University at St. Louise, U.S.A) (Yuan et al., 2003). *Slit1*$^{-/-}$; *Slit2*$^{-/-}$ double knockouts were generated by crossing *Slit1*$^{-/-}$ and *Slit2*$^{+/-}$ mice. *Robo1*$^{-/-}$ mice were obtained from Vasi Sundaresan and Bill Andrews (University College London, U.K.) (Andrews et al., 2006).

Immunohistochemistry

Embryos (E15–E17) were fixed via transcardial perfusion of 4% paraformaldehyde, after which brains were removed and sectioned at 45 μm coronally or sagittally on a vibratome. Sections were processed free-floating for immunohistochemistry as described previously (Campbell et al., 2008; Plachez et al., 2008). The primary antibodies used for immunohistochemistry were rabbit anti-GFAP (1:30,000; Z0334, Dako, Glostrup, Denmark); mouse anti-GAP 43 (1:100,000; AB1987, Chemicon, Temecula, CA), rabbit anti-GLAST (1:5000; a gift from Neils Danbolt, The University of Oslo) and rabbit anti-Robo1 (1:5000; a gift from Prof. Fujio Murakami, Osaka University). The colour reaction was performed in 3,3 diaminobenzidine (DAB) chromogen solution (2.5% nickel sulphate and 0.02% DAB in 0.175 M sodium acetate) activated with 0.01% (v/v) H_2O_2.

Dual in situ hybridisation and immunohistochemistry

In situ hybridisation was performed as described previously (Barry et al., 2008), followed by immunohistochemistry for rabbit anti-GFAP (1:30,000; Z0334; Dako; Glostrup, Denmark) as described above with minor modifications, where nickel sulphate was omitted from the colour reaction to achieve a contrasting brown precipitate. The riboprobes were a kind gift from Prof. Marc Tessier-Lavigne (Genetech).

Carbocyanine tract tracing

Tract tracing was performed as described previously (Piper et al., 2009a). Briefly, DiI (10% in dimethylformamide) was injected into the neocortex of E17 wildtype or *Slit1*$^{-/-}$; *Slit2*$^{-/-}$ mutant and wildtype mice using a picospritzer. Brains were stored in the dark at room temperature for a minimum of six weeks to allow dye diffusion, after which they were sectioned coronally at 45 μm on a vibratome. Injection sites were verified after sectioning by the presence of a fluorescent bolus and a needle track. Images were acquired using an ApoTome (Zeiss, Oberkochen, Germany) coupled to an upright fluorescence microscope (Zeiss Z1) and a digital camera (Zeiss AxioCam HRc).

Quantification and statistics

The distance of the corpus callosum, glial wedge and indusium griseum glia from the pial surface in wildtype, *Slit2*$^{-/-}$, and *Slit1*$^{-/-}$; *Slit2* mice was measured using ImageJ software (downloaded from http://rsbweb.nih.gov/ij/). The images were obtained using an upright microscope (Zeiss), after GFAP immunohistochemistry. The dorso-ventral height of the brain was also measured, and was used to normalise the distance of the glial structures to the pial surface in order to control for potential differences in brain size between genotypes. The data represent mean ± SD. Statistical analyses were performed using a two-tailed unpaired *t*-test.

In vitro collagen gel assay

Brains were dissected from litters of Robo1 mice from heterozygous matings that produced *Robo1*$^{+/+}$; *Robo1*$^{+/-}$ and *Robo1*$^{-/-}$ animals. E17 neocortex was dissected and chopped into approximately 300 μm square explants using a tissue chopper (McIlwain, Mickle Laboratory Engineering Co., Guildford, UK) and placed in collagen gels next to cell blocks. Cell blocks expressing Slit2 or control cells were generated by preparing a suspension of HEK-Slit2 stably transfected or vector-control transfected cells (a kind gift from Prof. Yi Rao, Wong et al., 2001) and then mixing the cells with 2% w/v low melting point agarose. The agar was allowed to set, after which the blocks of cells were cut and plated in collagen gels as previously described (Piper et al., 2009b; Shu and Richards, 2001). Collagen gels were grown without additional medium at 37 °C for 2 days in a humidified incubator. The cultures were then fixed, washed and stained for β-tubulin (TuJ1 clone, R&D Systems), after which they were imaged and analysed as previously described (Piper et al., 2009b). Briefly, the explants were imaged with deconvolution using an upright Axio-Imager Z1 (Zeiss) fitted with Apotome (Zeiss) to obtain all neurites in focus before flattening into a multiple image projection. The images were then quantified using a ridge-tracing algorithm (modified from Weaver et al., 2003) to detect neurite outgrowth. MatLab was used to post-process the images by identifying each explant's geometric centre, and then binning the traced neurite data into proximal and distal growth relative to the guidance factor source based on a directional marker annotated during imaging. A guidance ratio was obtained by comparing directed growth (proximal minus distal neurite pixels) with total outgrowth (total neurite pixels). Outgrowth was measured by normalising total growth (total neurite pixels) relative to explant size (total explant pixels). These measures provide control for growth-related effects and specifically allow measurement of directional guidance (Rosoff et al., 2004). Explants displaying poor growth (those with an outgrowth below one standard deviation of the mean) were eliminated from the experiment. Approximately 50 explants per condition, per experiment, were plated to ensure statistical significance. The data were then analysed using an unpaired Student's *t*-test. Differences were considered significant when $p<0.05$. Data are presented as average values for all samples pooled from at least three independent experiments per tissue ± standard error of the mean (SEM).

Diffusion magnetic resonance imaging and tractography

Following perfusion fixation and washes in phosphate buffered saline, diffusion-weighted (DW) images of E17 brains were acquired with the samples immersed in Fomblin Y-LVAC fluid (Solvay Solexis Italy), using a 16.4 T Bruker scanner and a 10 mm quadrature birdcage coil. A three-dimensional DW spin-echo sequence was acquired using the following parameters: repetition time = 400 ms; echo time = 22.8 ms; imaging resolution, 0.08 × 0.08 × 0.08 mm and a signal average of 1. Each dataset was composed of two B0 and thirty direction DW images (b value of 5000 s/mm^2; encoding gradient $\delta/\Delta = 2.5/14$ ms). Reconstruction and tractography were performed with Diffusion Toolkit (Ruopeng Wang and Van J. Wedeen. TrackVis.org, Martinos Center for Biomedical Imaging, Massachusetts General Hospital) according to high angular resolution diffusion (HARDI) and Q-ball models (Hess et al., 2006; Tuch, 2004; Tuch et al., 2003).

Tractography data were analysed using TrackVis, an interactive environment for fibre tracking reconstruction, display and analysis developed at the Martinos Center for Biomedical Imaging (www.trackvis.org). Wholebrain tractography was performed at fractional anisotropy values greater than 0.1 and a turning angle ≤ 45°. The complete track file was then graphically rendered for interactive three-dimensional display and analysis. Streamlines were generated from ROIs, which were manually outlined on colour-coded fractional anisotropy images.

Acknowledgements and funding

We thank Prof. Marc Tessier-Lavigne, Genentech, for providing riboprobes as well as the *Slit1*, *Slit2* and *Slit1/2* mutant mice and for supplying the *Slit3* mutant mice that were generated and provided with permission by Prof. David Ornitz, Washington University, St Louis. We thank Dr. Vasi Sundaresan and Dr. Bill Andrews, Kings College London and University College London, for providing the *Robo1*$^{-/-}$ mice, Dr. Niels Danbolt for the GLAST antibody and Prof. Fujio Murakami for the Robo1 antibody. We are grateful to Rowan Tweedale for critical reading of the manuscript and for members of the Goodhill Laboratory (Queensland Brain Institute) for their assistance in the analysis of the explant assay. This work was supported by grants 456026 and 631466 to LJR and 456040 to HC and LJR from the National Health and Medical Research Council (NHMRC) of Australia. MP is supported by a Career Development Award and LJR is supported by a Principal Research Fellowship from the NHMRC. HC is supported by a Smart State Fellowship from the Queensland Government. DU was supported by University of Queensland International Post Graduate and International Living Allowance Scholarships, IG was supported by a University of Queensland Research Scholarship and ALSD was supported by an Australian Postgraduate Research Award.

References

Andrews, W., Liapi, A., Plachez, C., Camurri, L., Zhang, J., Mori, S., Murakami, F., Parnavelas, J.G., Sundaresan, V., Richards, L.J., 2006. Robo1 regulates the development of major axon tracts and interneuron migration in the forebrain. Development 133, 2243–2252.

Bagri, A., Marin, O., Plump, A.S., Mak, J., Pleasure, S.J., Rubenstein, J.L., Tessier-Lavigne, M., 2002. Slit proteins prevent midline crossing and determine the dorsoventral position of major axonal pathways in the mammalian forebrain. Neuron 33, 233–248.

Barresi, M.J., Hutson, L.D., Chien, C.B., Karlstrom, R.O., 2005. Hedgehog regulated Slit expression determines commissure and glial cell position in the zebrafish forebrain. Development 132, 3643–3656.

Barry, G., Piper, M., Lindwall, C., Moldrich, R., Mason, S., Little, E., Sarkar, A., Tole, S., Gronostajski, R.M., Richards, L.J., 2008. Specific glial populations regulate hippocampal morphogenesis. J. Neurosci. 28, 12328–12340.

Bignami, A., Dahl, D., 1974. Astrocyte-specific protein and radial glia in the cerebral cortex of newborn rat. Nature 252, 55–56.
Brose, K., Bland, K.S., Wang, K.H., Arnott, D., Henzel, W., Goodman, C.S., Tessier-Lavigne, M., Kidd, T., 1999. Slit proteins bind Robo receptors and have an evolutionarily conserved role in repulsive axon guidance. Cell 96, 795–806.
Campbell, C.E., Piper, M., Plachez, C., Yeh, Y.T., Baizer, J.S., Osinski, J.M., Litwack, E.D., Richards, L.J., Gronostajski, R.M., 2008. The transcription factor Nfix is essential for normal brain development. BMC Dev. Biol. 8, 52.
Gobius, I., Richards, L.J., 2011. Creating connections in the developing brain: Mechanisms regulating corpus collosum development. In: McCarthy, M.M. (Ed.), Colloquium Series in the Developing Brain. Morgan & Claypool Lifesciences, New Jersey, pp. 1–48.
Hartfuss, E., Galli, R., Heins, N., Gotz, M., 2001. Characterization of CNS precursor subtypes and radial glia. Dev. Biol. 229, 15–30.
Hess, C.P., Mukherjee, P., Han, E.T., Xu, D., Vigneron, D.B., 2006. Q-ball reconstruction of multimodal fiber orientations using the spherical harmonic basis. Magn. Reson. Med. 56, 104–117.
Islam, S.M., Shinmyo, Y., Okafuji, T., Su, Y., Naser, I.B., Ahmed, G., Zhang, S., Chen, S., Ohta, K., Kiyonari, H., Abe, T., Tanaka, S., Nishinakamura, R., Terashima, T., Kitamura, T., Tanaka, H., 2009. Draxin, a repulsive guidance protein for spinal cord and forebrain commissures. Science 323, 388–393.
Jaworski, A., Long, H., Tessier-Lavigne, M., 2010. Collaborative and specialized functions of Robo1 and Robo2 in spinal commissural axon guidance. J. Neurosci. 30, 9445–9453.
Jones, D., Cercignani, K.M., 2010. Twenty-five pitfalls in the analysis of diffusion MRI data. NMR Biomed. 23, 803–820.
Keeble, T.R., Halford, M.M., Seaman, C., Kee, N., Macheda, M., Anderson, R.B., Stacker, S.A., Cooper, H.M., 2006. The Wnt receptor Ryk is required for Wnt5a-mediated axon guidance on the contralateral side of the corpus callosum. J. Neurosci. 26, 5840–5848.
Kidd, T., Bland, K.S., Goodman, C.S., 1999. Slit is the midline repellent for the robo receptor in *Drosophila*. Cell 96, 785–794.
Koester, S.E., O'Leary, D.D., 1994. Axons of early generated neurons in cingulate cortex pioneer the corpus callosum. J. Neurosci. 14, 6608–6620.
Lindwall, C., Fothergill, T., Richards, L.J., 2007. Commissure formation in the mammalian forebrain. Curr. Opin. Neurobiol. 17, 3–14.
Lopez-Bendito, G., Flames, N., Ma, L., Fouquet, C., Di Meglio, T., Chedotal, A., Tessier-Lavigne, M., Marin, O., 2007. Robo1 and Robo2 cooperate to control the guidance of major axonal tracts in the mammalian forebrain. J. Neurosci. 27, 3395–3407.
Marillat, V., Cases, O., Nguyen-Ba-Charvet, K.T., Tessier-Lavigne, M., Sotelo, C., Chedotal, A., 2002. Spatiotemporal expression patterns of slit and robo genes in the rat brain. J. Comp. Neurol. 442, 130–155.
Mendes, S.W., Henkemeyer, M., Liebl, D.J., 2006. Multiple Eph receptors and B-class ephrins regulate midline crossing of corpus callosum fibers in the developing mouse forebrain. J. Neurosci. 26, 882–892.
Moldrich, R.X., Pannek, K., Hoch, R., Rubenstein, J.L., Kurniawan, N.D., Richards, L.J., 2010. Comparative mouse brain tractography of diffusion magnetic resonance imaging. Neuroimage 51, 1027–1036.
Nguyen-Ba-Charvet, K.T., Plump, A.S., Tessier-Lavigne, M., Chedotal, A., 2002. Slit1 and slit2 proteins control the development of the lateral olfactory tract. J. Neurosci. 22, 5473–5480.
Niquille, M., Garel, S., Mann, F., Hornung, J.P., Otsmane, B., Chevalley, S., Parras, C., Guillemot, F., Gaspar, P., Yanagawa, Y., Lebrand, C., 2009. Transient neuronal populations are required to guide callosal axons: a role for semaphorin 3C. PLoS Biol. 7, e1000230.
Ozaki, H.S., Wahlsten, D., 1992. Prenatal formation of the normal mouse corpus callosum: a quantitative study with carbocyanine dyes. J. Comp. Neurol. 323, 81–90.
Paul, L.K., Brown, W.S., Adolphs, R., Tyszka, J.M., Richards, L.J., Mukherjee, P., Sherr, E.H., 2007. Agenesis of the corpus callosum: genetic, developmental and functional aspects of connectivity. Nat. Rev. Neurosci. 8, 287–299.
Piper, M., Barry, G., Hawkins, J., Mason, S., Lindwall, C., Little, E., Sarkar, A., Smith, A.G., Moldrich, R.X., Boyle, G.M., Tole, S., Gronostajski, R.M., Bailey, T.L., Richards, L.J., 2010. NFIA controls telencephalic progenitor cell differentiation through repression of the Notch effector Hes1. J. Neurosci. 30, 9127–9139.
Piper, M., Dawson, A.L., Lindwall, C., Barry, G., Plachez, C., Richards, L.J., 2007. Emx and Nfi genes regulate cortical development and axon guidance in the telencephalon. Novartis Found. Symp. 288, 230–242 (discussion 242–5, 276–81).
Piper, M., Moldrich, R.X., Lindwall, C., Little, E., Barry, G., Mason, S., Sunn, N., Kurniawan, N.D., Gronostajski, R.M., Richards, L.J., 2009a. Multiple non-cell-autonomous defects underlie neocortical callosal dysgenesis in Nfib-deficient mice. Neural Dev. 4, 43.
Piper, M., Plachez, C., Zalucki, O., Fothergill, T., Goudreau, G., Erzurumlu, R., Gu, C., Richards, L.J., 2009b. Neuropilin 1-Sema signaling regulates crossing of cingulate pioneering axons during development of the corpus callosum. Cereb. Cortex 19 (Suppl. 1), i11–i21.
Plachez, C., Lindwall, C., Sunn, N., Piper, M., Moldrich, R.X., Campbell, C.E., Osinski, J.M., Gronostajski, R.M., Richards, L.J., 2008. Nuclear factor I gene expression in the developing forebrain. J. Comp. Neurol. 508, SPC1.
Plump, A.S., Erskine, L., Sabatier, C., Brose, K., Epstein, C.J., Goodman, C.S., Mason, C.A., Tessier-Lavigne, M., 2002. Slit1 and Slit2 cooperate to prevent premature midline crossing of retinal axons in the mouse visual system. Neuron 33, 219–232.
Rash, B.G., Richards, L.J., 2001. A role for cingulate pioneering axons in the development of the corpus callosum. J. Comp. Neurol. 434, 147–157.
Ren, T., Zhang, J., Plachez, C., Mori, S., Richards, L.J., 2007. Diffusion tensor magnetic resonance imaging and tract-tracing analysis of Probst bundle structure in Netrin1- and DCC-deficient mice. J. Neurosci. 27, 10345–10349.
Richards, L.J., 2002. Axonal pathfinding mechanisms at the cortical midline and in the development of the corpus callosum. Braz. J. Med. Biol. Res. 35, 1431–1439.
Rosoff, W.J., Urbach, J.S., Esrick, M.A., McAllister, R.G., Richards, L.J., Goodhill, G.J., 2004. A new chemotaxis assay shows the extreme sensitivity of axons to molecular gradients. Nat. Neurosci. 7, 678–682.
Sánchez-Camacho, C., Ortega, J.A., Ocaña, I., Alcántara, S., Bovolenta, P., 2011. Appropriate Bmp7 levels are required for the differentiation of midline guidepost cells involved in corpus callosum formation. Dev. Neurobiol. 71, 337–350.
Shu, T., Richards, L.J., 2001. Cortical axon guidance by the glial wedge during the development of the corpus callosum. J. Neurosci. 21, 2749–2758.
Shu, T., Butz, K.G., Plachez, C., Gronostajski, R.M., Richards, L.J., 2003a. Abnormal development of forebrain midline glia and commissural projections in Nfia knock-out mice. J. Neurosci. 23, 203–212.
Shu, T., Puche, A.C., Richards, L.J., 2003b. Development of midline glial populations at the corticoseptal boundary. J. Neurobiol. 57, 81–94.
Shu, T., Sundaresan, V., McCarthy, M.M., Richards, L.J., 2003c. Slit2 guides both precrossing and postcrossing callosal axons at the midline in vivo. J. Neurosci. 23, 8176–8184.
Silver, J., Edwards, M.A., Levitt, P., 1993. Immunocytochemical demonstration of early appearing astroglial structures that form boundaries and pathways along axon tracts in the fetal brain. J. Comp. Neurol. 328, 415–436.
Smith, K.M., Ohkubo, Y., Maragnoli, M.E., Rasin, M.R., Schwartz, M.L., Sestan, N., Vaccarino, F.M., 2006. Midline radial glia translocation and corpus callosum formation require FGF signaling. Nat. Neurosci. 9, 787–797.
Tuch, D.S., 2004. Q-ball imaging. Magn. Reson. Med. 52, 1358–1372.
Tuch, D.S., Reese, T.G., Wiegell, M.R., Wedeen, V.J., 2003. Diffusion MRI of complex neural architecture. Neuron 40, 885–895.
Weaver, C.M., Pinezich, J.D., Lindquist, W.B., Vazquez, M.E., 2003. An algorithm for neurite outgrowth reconstruction. J. Neurosci. Methods 124, 197–205.
Wong, K., Ren, X.R., Huang, Y.Z., Xie, Y., Liu, G., Saito, H., Tang, H., Wen, L., Brady-Kalnay, S.M., Mei, L., Wu, J.Y., Xiong, W.C., Rao, Y., 2001. Signal transduction in neuronal migration: roles of GTPase activating proteins and the small GTPase Cdc42 in the Slit-Robo pathway. Cell 107, 209–221.
Wise, S.P., Jones, E.G., 1976. The organization and postnatal development of the commissural projection of the rat somatic sensory cortex. J. Comp. Neurol. 168, 313–343.
Yuan, W., Rao, Y., Babiuk, R.P., Greer, J.J., Wu, J.Y., Ornitz, D.M., 2003. A genetic model for a central (septum transversum) congenital diaphragmatic hernia in mice lacking Slit3. Proc. Natl. Acad. Sci. U. S. A. 100, 5217–5222.